energies

MDPI

Article

Elements of Transition-State Theory in Relation to the Thermal Dissociation of Selected Solid Compounds

Andrzej Mianowski, Tomasz Radko and Rafał Bigda *

Institute of Energy and Fuel Processing Technology, Zamkowa 1, 41-803 Zabrze, Poland
* Correspondence: rbigda@itpe.pl

Abstract: An analysis was carried out on the thermal dissociation of selected inorganic salts according to Transition-State Theory (TST). For this purpose, two possibilities were compared in the context of rate constants: in the first case using the Arrhenius constant directly from TST, and in the second, using the thermodynamic equilibrium constant of the reaction/process of active state formation. The determined relationships are presented in the form of temperature profiles. It was established that TST applies to reactions for which there is a formally and experimentally reversible reaction, in the literal sense or catalytic process. The importance of the isoequilibrium temperature, which results from the intersection of the thermodynamic temperature profile and the Gibbs free energy of activation, was demonstrated. Its values close to the equilibrium temperature are indicative of more dynamic kinetic qualities. As part of the discussion, the Kinetic Compensation Effect (KCE) was used to observe changes in the entropy of activation by comparing two kinetic characteristics of the same reaction. Enthalpy–Entropy Compensation (EEC) was shown to be the same law as KCE, just expressed differently. This was made possible by TST, specifically the entropy of activation at isokinetic temperature, by which the perspective of the relationship of energy effects changes.

Keywords: solid state; Transition-State Theory (TST); reversible reactions; phenomenological thermodynamics; activation temperature; isoequilibrium temperature; isokinetic temperature

check for updates

Citation: Mianowski, A.; Radko, T.; Bigda, R. Elements of Transition-State Theory in Relation to the Thermal Dissociation of Selected Solid Compounds. *Energies* **2024**, *17*, 2669. https://doi.org/10.3390/en17112669

Academic Editor: Jiro Senda

Received: 24 April 2024
Revised: 23 May 2024
Accepted: 28 May 2024
Published: 30 May 2024

Copyright: © 2024 by the authors. Licensee MDPI, Basel, Switzerland. This article is an open access article distributed under the terms and conditions of the Creative Commons Attribution (CC BY) license (https://creativecommons.org/licenses/by/4.0/).

1. Introduction and Aim of the Work

In 1935, Eyring proposed a kinetic theory called Transition-State Theory (TST), which deals with the kinetics of elementary reactions in the gas phase and then in the liquid phase [1].

A monograph analyzing TST (comprising 843 entries) was published in 1996, with little discussion of the use of this theory for solid-phase thermal dissociation processes. TST has been widely used for the calculation and analysis of rate constants for chemical reactions in a variety of condensed-phase systems such as liquids, solids, and gas–solids [2]. Of the items cited there, the 1937 concept [3], sometimes referred to as the Eyring–Evans–Polanyi model, is the most common, and the possibility of applying it to the solid phase was presented in 1964 by Shannon [4]. In a subsequent discussion paper in 2000 [5] the condensed phase is reduced to a liquid phase.

Despite the lack of explicit recommendations, the TST is used without much trouble compared to the classical Arrhenius law, and moreover, for the isoconversion methods used for each conversion level. Knowing the activation energy and pre-exponential constant at each node, the temperature of formation of the active complex is taken as the temperature of the maximum reaction/process rate. Works are found on multi-step analyses of heterogeneous solids, e.g., polymers with rice husks ash (as a catalyst) [6] or with oils [7], and also on the thermal decomposition of biomass with possible additives [8–16]. TST models refer to kinetic parameters determined classically for a constant heating rate [7,8], but sometimes for isoconversion methods (Vyazovkin, Friedman, FWO, KAS, Starink and others), i.e., for constant transformation step levels [9–14,16] or over specific temperature ranges [8,15]. In

the latter case, the Arrhenius law parameters, i.e., activation energy (E) and pre-exponential factor ($\ln A$), are determined for each transformation step, but the validity of the temperature assumed in the TST model remains a matter of debate. The temperature of the maximum reaction/process rate, determined under conditions for a linear temperature increase and used in the Kissinger equation, is most commonly adopted [17]. According to the literature, the TST model assumes the temperature at which the tests are conducted. This leads to the conclusion that these are processes studied under isothermal conditions.

The literature review indicates a clear gap in the interpretation of solid-phase thermal dissociation using TST. The aim of this study is to analyze the feasibility of using TST to confront the thermodynamic temperature profiles of free, phenomenological, and activation energy for selected solid salts. The temperature profiles were determined for specific temperature ranges, but their range was logically extended for interpretative purposes. Thermal dissociation kinetics were related to the Arrhenius equation, not necessarily only under isothermal conditions.

A partial aim is to seek a link between the phenomenological thermodynamics approach and activation thermodynamics.

2. Relation between Arrhenius Law and TST

An analysis of the literature [18–35] which studies the relations between the classical Arrhenius equation and TST, i.e., the connection between kinetics and thermodynamics, allows us to present a concept for the relation in question.

We analyze the course of an isothermal reaction (T = const) of a solid-state chemical substance. In the first step we assume a first-order reversible reaction pathway. In this case, the equilibrium constant is derived from the ratio of the rate constants of the forwards to backwards reactions:

$$K = \frac{k_1}{k_{-1}} \tag{1}$$

The transition of the reactant to the TST state can be imagined as an endoenergetic process of thermal activation, where, as a result of the relaxation of the structure, a gas product is released and at least two reactants, a solid phase and a reactive gas, can be considered to appear. Thus, the postulate that this is a gas–solid interface system is fulfilled [2].

A comparison of kinetic constants according to Arrhenius and TST assumes equality:

$$k_{exp} = k_{TST} \tag{2}$$

The right-hand side of Equation (1), on the other hand, is a typical TST notation which, according to some works [1–5,18–35] and other extremely helpful ones [36–47] containing additional knowledge and comments, can be written as:

$$k_{TST} = \chi \cdot k^+ \cdot K^+ = \chi \cdot \frac{\mathrm{k_B} T}{h} \cdot \exp\left(-\frac{\Delta G^+}{\mathrm{R}T}\right) \tag{3}$$

where:

$$\Delta G^+ = \Delta H^+ - T\Delta S^+ \tag{4}$$

and the ratio of Boltzmann's and Planck's constants is a constant quantity equal to $B = \frac{\mathrm{k_B}}{h} = 2.0836 \times 10^{10}\ \mathrm{K^{-1}\ s^{-1}}$, and we tacitly assume that we are comparing Arrhenius' law with TST for $\chi = 1$, which is consistent with many views, and this problem will be returned to in the discussion of the results.

We write the ratio in Equation (2) as:

$$k_{exp} = k^+ \cdot K^+ \tag{5}$$

whereby in the reference to Equation (2) the left-hand side is written as:

$$k_{exp} = A\exp\left(-\frac{E}{\mathrm{R}T}\right) \tag{6}$$

Formally we assume $k = k_{exp} = A\exp\left(-\frac{E}{\mathrm{R}T}\right)$, with the new parameter constants of the Arrhenius equation being the resultant of the constants from the individual reaction steps. This raises the issue of whether, for thermal dissociation of the solid phase, it is correct to insert the temperature of the maximum reaction rate T_m, determined dynamically, into the subsequent equations. According to the Kissinger equation [17], the temperature of the maximum reaction rate increases with the heating rate. For very high heating rates and for P = 0.1 MPa, $T_m \rightarrow T_{eq}$ [48]. However, it is advisable not to exceed the product of the mass of the sample and heating rate of 100 mg K·min^{-1}, or better yet, the product of the time constant and heating rate below 2–3 K [49].

Using the proposal of Evans and Polanyi [3] comparing Equation (5) with (6) using Equation (3) after bilateral logarithmization:

$$\ln A - \frac{E}{\mathrm{R}T} = \ln \mathrm{B}T - \frac{\Delta G^+}{\mathrm{R}T},\ \chi = 1 \tag{7}$$

and after differentiation with respect to temperature we obtain:

$$\frac{E}{\mathrm{R}T^2} = \frac{1}{T} + \frac{\Delta H^+}{\mathrm{R}T^2} \tag{8}$$

which leads to a well-known relationship:

$$E = \mathrm{R}T + \Delta H^+ \tag{9}$$

In the literature, Equation (9) is presented as [37]:

$$\Delta H^+ = E - n\mathrm{R}T \tag{10}$$

in which: n = 0 applies to phenomena of physical nature (polymorphic transformations, glass transition) and polymerization [50], n = 1 is valid for single-molecule reactions, and n = 2 is recommended for two-molecule reactions. Thus, for solid-phase dissociation, Equation (9) is the most reasonable.

The Gibbs energy of the activation process follows from Equation (3):

$$\Delta G^+ = E + \mathrm{R}T\ln\left(\frac{\mathrm{B}T}{A}\right) \tag{11}$$

what is equivalent in case of availability to the rate constant according to Arrhenius or the diffusion coefficient in s^{-1}:

$$\Delta G^+ = \mathrm{R}T\ln\left(\frac{\mathrm{B}T}{k}\right) \tag{12}$$

The entropy of activation follows from the formulae Equations (10) and (12):

$$\Delta S^+ = \frac{\Delta H^+ - \Delta G^+}{T} \tag{13}$$

and after arranging we obtain:

$$\Delta S^+ = \mathrm{R}\left[\ln\left(\frac{A}{\mathrm{B}T}\right) - 1\right],\quad n = 1 \tag{14}$$

If we insert in Equation (14) the expression defined in [30] as 'Yard Stick':

$$A = \mathrm{B}T\mathrm{e} \tag{15}$$

we determine $\Delta S^{+} = 0$, otherwise, entropy neutral.

For n = 0, Equation (14) simplifies to the form: $\Delta S^{+} = \mathrm{R}\ln\left(\frac{A}{\mathrm{B}T}\right)$ [50].

If $A < \mathrm{B}T\mathrm{e}$, the entropy of activation is negative $\Delta S^{+} < 0$, which is characteristic of slow reactions and when the entropy of the TST state with respect to the reactants decreases [35], which is related to a higher ordering, under certain constraints the slowdown can be explained based on RRKM theory [51]. Equation (14) is derived by differentiating Equation (11) with respect to temperature.

One further observation, ignoring other constraints, is that if we consider $T = T_m = \text{const.}$ in Equation (14), then the entropy of activation is proportional to $\ln A$ [9] and even to E.

3. The Concept Based on the Equilibrium Constant According to Equation (1)

The key element is Equation (1). Equilibrium constant of the reaction with the very important caveat postulated for thermal dissociation of the solid phase, that K varies between $0 < K \leq 1$:

$$\ln K = -\frac{\Delta_r G^{\varnothing}}{\mathrm{R}T},\ \Delta_r G^{\varnothing} = 0 \text{ and } T = T_{eq} = \frac{\Delta_r H^{\varnothing}}{\Delta_r S^{\varnothing}} \gg 0 \tag{16}$$

After bilateral logarithmization of Equation (1):

$$\ln K = \ln k_1 - \ln k_{-1} \tag{17}$$

and using Equation (16) for the left-hand side of Equations (17) and (12) for the right-side twice, we obtain:

$$\Delta_r G^{\varnothing} = \Delta G^{+} - \Delta_{-1}\, G^{+} \tag{18}$$

Equation (18) is the simplest approach linking phenomenological thermodynamics to activation thermodynamics and at least two conditions are relevant.

Firstly, in Equation (18) for equilibrium condition $\Delta_r G^{\varnothing} = 0$, the equality occurs:

$$\Delta G^{+} = \Delta_{-1}\, G^{+}\big|_{T=T_{eq}} \tag{19}$$

that is valid for $K = 1$, since $k_1 = k_{-1}$, therefore for $T > T_{eq}$ activation loses its meaning.

Using Equation (18) twice for the decomposition (k_1) and synthesis (k_{-1}) reactions, we obtain:

$$\begin{aligned} \Delta_r G^{\varnothing} &= \Delta G^{+} - \Delta_{-1} G^{+} \quad \text{decomposition, Equation (18)} \\ -\Delta_r G^{\varnothing} &= \Delta_{-1} G^{+}_{exp} - \Delta G^{+} \qquad \text{synthesis} \end{aligned} \tag{20}$$

and we come to a comparison:

$$\Delta_{-1} G^{+}_{exp} = \Delta_{-1} G^{+} \tag{21}$$

For Equation (21) there is at least one common temperature, although perfect agreement cannot be ruled out.

Secondly, from Equation (18) we obtain two comparison possibilities at isoequilibrium temperature:

$$\Delta_r G^{\varnothing} = \Delta G^{+}\big|_{T=T_K} \tag{22}$$

and acc. Equation (19):

$$\Delta_r G^{\varnothing} = \Delta_{-1} G^{+}\big|_{T=T_{-K}} \tag{23}$$

while: $T_K < T_{-K}$.

While according to Equation (19) there is a common equilibrium temperature (T_{eq}) for forward and backward activation reactions, the common coordinates according to Equations (22) and (23) correspond to temperatures T_{-K} and, of lesser cognitive importance, T_{-K}, respectively, determining the local isoequilibrium.

In accordance with Equation (21), it determines the temperature isoequilibrium for the experimental data:

$$\Delta_r G^{\varnothing} = \Delta_{-1} G^{+}_{exp}\Big|_{T=T_{-K}} \tag{24}$$

Equations (23) and (24) are meaningful when we have a kinetic description of the reaction reversible to its decomposition.

The common temperature for coordinates T_K with respect to $\Delta_r G^{\varnothing}$ correspond to the expected partial objectives. Using calculations from Equation (22), the equilibrium constant of the activation process can be determined from standard thermodynamic data at this temperature T_K:

$$\mathrm{R}\ln\ K^{+} = \Delta_r S^{\varnothing} - \frac{\Delta_r H^{\varnothing}}{T_K} \tag{25}$$

From Equation (25), it follows that the quantities K^{+} are infinitesimally small but greater than 0; however, two facts should be noted: T_K may not appear at all in the real temperature range, or it may exist as an intersection point between the straight line of the thermodynamic relation and the activation process for backward reaction as T_{-K}.

4. Examples of Analysis Using Equation (1)

4.1. Formal Assumptions

The basic assumption is that there is a linear relationship of the free energies, ΔG^{+} vs. $\Delta_r G^{\varnothing}$, which in turn allows the temperature profiles of each energy to be analysed separately.

A summary for several dissociation reactions of solid reactants is presented in Table 1. On the basis of data collected in work [52], the relationships, composed of average thermodynamic quantities, were calculated:

$$\Delta_r G^{\varnothing} = a_0 - a_1 T,\ \ \mathrm{kJ{\cdot}mol^{-1}} \tag{26}$$

and for the known Arrhenius law parameters, the relationships were determined:

$$\Delta G^{+} = a_2 + a_3 T,\ \mathrm{kJ{\cdot}mol^{-1}} \tag{27}$$

In Equations (26) and (27), the dimension $\mathrm{kJ{\cdot}mol^{-1}}$ denotes the quantity related to 1 mole of reactant.

Equation (27) follows from the aforementioned basic assumption, when accepting the linear relationship (26) [52]. It represents a form of linear relationship with respect to temperature (previously incorporating the term RTln T) using Equation (4) which is more appropriate for these procedures than Equation (12).

According to the assumptions made, the constants in Equations (26) and (27) are average thermodynamic quantities, approximating for $T = 298$ K, $a_0 \cong \Delta_{298} H^{\varnothing}$, $a_1 \cong \Delta_{298} S^{\varnothing}$ and we can make a similar comparison as $a_2 \cong \Delta H^{+}$, $a_3 \to -\Delta S^{+}$. The notation $\Delta G^{+} \cong \Delta H^{+} - (-\Delta S^{+})T$ indicates the usually observed negative entropy of activation, which follows from Equation (15) when $A < \mathrm{B}T\mathrm{e}$.

The coefficients of the equations are given in Table 1, and the values of the standard thermodynamic functions ($T = 298$ K) given therein sufficiently explain the meaning of the calculated coefficients a_0 and a_1.

Table 1. List of analyzed chemical reactions and numerical data for determining the activation and standard free energy with respect to temperature (the dimension kJ·mol^{-1} denotes the quantity related to 1 mole of reactant, the values calculated according to [52] were supplemented by other ones [53–57]).

Reaction/Temperature Range P **= 0.1 MPa**	$\Delta_r G^{\emptyset} = a_0 - a_1 \cdot T$ **kJ·mol^{-1}**		$\Delta G^{+} = a_2 + a_3 \cdot T$ **kJ·mol^{-1}**		E **kJ·mol^{-1}**	ln$A$ A **in s^{-1}**	$\Delta_{298} H^{\emptyset}$ [52] **kJ·mol^{-1}**	$\Delta_{298} S^{\emptyset}$ [52] **J·mol^{-1}·K^{-1}**
	a_0	a_1	a_2	a_3				
$CaCO_3^{(s)} = CaO^{(s)} + CO_2^{(g)}$ calcite, T = 298–1200 K	174.92 [52]	0.150 [52]	185.55	0.132	191.0 [53]	15.40 [53]	178.3	158.9
$Fe_2(SO_4)_3^{(s)} = Fe_2O_3^{(s)} + 3SO_3^{(g)}$ hematite, T = 298–1200 K	566.41 [52]	0.538 [52]	-	-	-	-	571.4	550.2
	582.39 [54]	0.557 [54]	209.73	0.048	218.4	25.84		
					823–923 K [56]			
	526.51 [55]	0.501 [55]	74.40	0.253	83.3	1.33		
					973–1123 K [55]			
$Al_2(SO_4)_3^{(s)} = \gamma\text{-}Al_2O_3^{(s)} + 3SO_3^{(g)}$ T = 900–1250 K	610.90 [54]	0.534 [54]	258.92	0.105	267.8	19.06	596.6	583.3
					923–1223 K [55]			
$2AgNO_3^{(s)} = 2Ag^{(s)} + O_2^{(g)} + 2NO_2^{(g)}$ T = 298–600 K	156.47 [52]	0.241 [52]	124.94	0.132	129.2 [57]	15.20 [57]	157.5	244.7
$4NH_4ClO_4^{(s)} = 4HCl^{(g)} + 2N_2^{(g)} + 5O_2^{(g)} + 6H_2O^{(g)}$ T = 298–500 K	−159.98 [52]	0.636 [52]	96.83	0.048	100.0 [53]	25.0 [53]	−159.3	638.4
$2NH_4ClO_4^{(s)} = Cl_2^{(g)} + N_2^{(g)} + 2O_2^{(g)} + 4H_2O^{(g)}$ T = 298–500 K	−188.78 [52]	0.603 [52]					−187.9	606.3

Based on the data summarized in Table 1, the temperature profiles of the thermal dissociation processes of the exemplary compounds were determined. For the selected examples shown in Figures 1–5, the profiles are annotated accordingly:

- Equation (26), $\Delta_r G^{\varnothing}$—line 1,
- Equation (27), ΔG^{+}—line 2,
- Equation (26) after reversal of the signs $(-\Delta_r G^{\varnothing})$—line 3,
- Equation (12) for experimental data of the activation state of a reversible reaction, $\Delta_{-1} G^{+}$ (line 4a), represented by the results of experimental studies, $\Delta_{-1} G^{+}_{exp}$, (line 4b),
- other, explained for the specific example—line 5.

While according to Equations (26) and (27) these are linear relationships with respect to temperature, also according to Equation (18) an identical mathematical structure can be expected for $\Delta_{-1}\ G^{+}$. However, it is not always experimentally possible to control this option. As an approximation, a simplification can be adopted to facilitate the interpretation of Equation (18). The reversible reaction (represented as line 3) as an activation process can be written directly. This is a special case of Equation (18) at temperature T_{eq}, where for example $C = \Delta G^{+}\left(T_{eq}\right) = \text{const}$ (option '0'):

$$\Delta_{-1} G^{+} \cong -\Delta_r G^{\varnothing} + \mathrm{C} \tag{28}$$

Going further, inserting directly ΔG^{+} instead of constant C, Equation (18) is reproduced.

The equality of Equations (26) and (27) determines the isoequilibrium temperature T_K ($\Delta_r G^{\varnothing} = \Delta G^{+}$, Equation (22)) and in some cases T_{-K} (Equation (23) or Equation (24)) which will be discussed further for several examples (Appendix A.1). Figures 1–5 are the free energy temperature profiles with the characteristic temperatures marked.

4.2. Calcite

The thermal decomposition of limestone follows the equation:

$$\mathrm{CaCO_3}^{\mathrm{s}} \leftrightarrow \mathrm{CaO}^{\mathrm{s}} + \mathrm{CO_2}^{\mathrm{g}} \tag{29}$$

Formally, this is a reversible reaction whose course depends on the physical properties of the calcium oxide. It is therefore possible to compare the typical geometrical structure for these considerations, comprising Equations (26) and (27) and the experimental data for the carbonation reaction. The different straight lines denote the temperature profiles for the chemical reactions shown in Table 1. In Figure 1, lines 1 to 3 and 4a,b denote the equations given in the summary (sub-point 4.1), while line 4b corresponds for the experimental data from three sources [58–60] for the reversible reaction according to Equation (12). From Equation (18), the missing form of the equation follows, i.e., $\Delta_{-1} G^{+}$ = 10.63 + 0.282T (line 4a) consistent with Equation (19) for T_{eq}= 1166.13 K.

The kinetics of diffusion processes according to the RPM model for the same data are distinguished [60]. Line 4b is common to all the experimental activation data of the reversible reaction; it intersects lines 2 and 4a,b in the closest neighborhood of the isokinetic temperature (T_{eq}), which can be considered a very satisfactory result.

The geometry of the temperature profiles, including all the straight lines, indicates a preference for equilibrium temperature, since according to these considerations when $\Delta_r G^{\varnothing}$ = 0.

If $T > T_{eq}$ (line 3) the possibility of an activation-reversible reaction disappears. This is in accordance with the experimental data and lines 4a and 4b are very close, although their coefficients differ slightly.

The coefficients of lines 2 and 4a,b are dependent on the reaction kinetics, and thus the isoequilibrium temperature T_K or T_{-K} is strongly variable.

This example illustrates the possibility of considering the product of a thermal dissociation reaction as either capable of a reversible reaction, or with variable weaker reactivity in this respect.

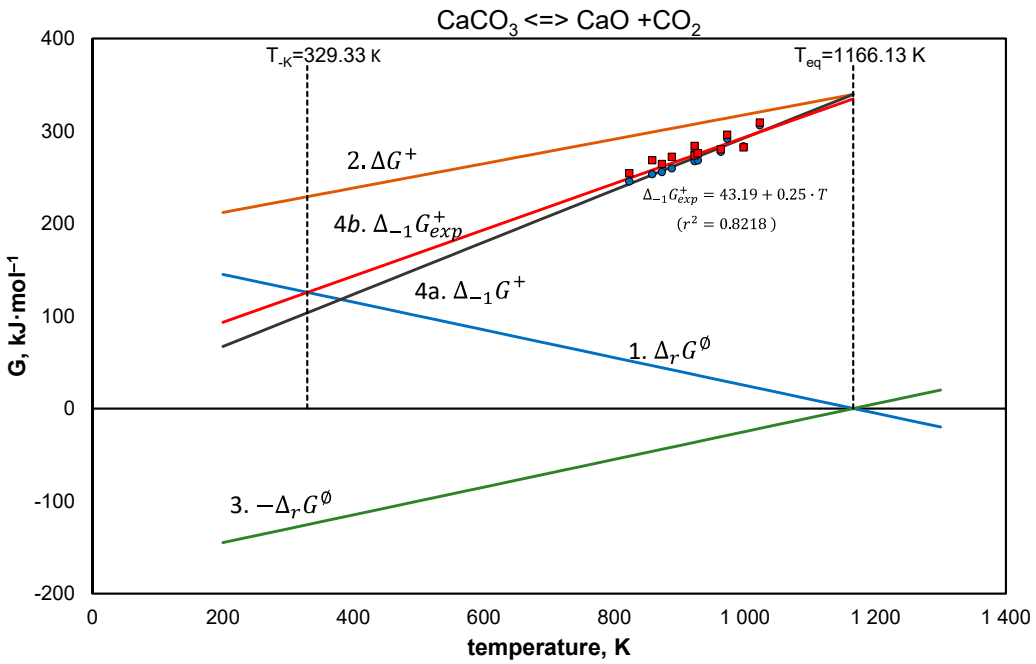


Figure 1. Thermodynamic analysis of the course of the $CaCO_3 \leftrightarrow CaO + CO_2$ reaction, Equation (29). In the reference to Equation (18), line 4a is a straight line: $\Delta_{-1}G^{+} = 10.63 + 0.282 \cdot T$. For line 4b the resultant Gibbs free energy calculated for the diffusion coefficient (red squares) and the kinetic constant (blue circles) was taken. Equation (12) was used with the Arrhenius parameter calculation omitted, the equation of line 4b is given in the graph. The other kinetic data were determined for dynamic conditions; T_{eq} = 1166.13 K, T_K = does not exist, from comparison $\Delta_r G^{\varnothing} = \Delta_{-1} G^{+}$ we obtain T_{-K} = 380.30 K—line 4a, and from $\Delta_r G^{\varnothing} = \Delta_{-1} G^{+}_{exp}$, T_{-K} = 329.33 K—line 4b.

4.3. Iron(III) Sulphate (Ferric Sulphate)

For reaction in this form:

$$Fe_2(SO_4)_3{}^{s} \leftrightarrow Fe_2O_3{}^{s} + 3SO_3{}^{g} \tag{30}$$

in sulphate decomposition studies, in which the cation is a metal, there can be a temperature-dependent reduction in SO_3:

$$SO_3 \leftrightarrow SO_2 + 1/2O_2 \tag{31}$$

In this case, hematite is considered as the reaction (30) catalyst in the course of the reversible reaction (31) [61,62]. In Table 1, a reference to the formation of SO_3 is assumed in the thermodynamic range:

$$\Delta_r G^{\varnothing} = 566.41 - 0.538 \cdot T, \quad \text{kJ} \cdot \text{mol}^{-1}, \quad \text{for } SO_3 \tag{32}$$

The reactions (30) with (31) form a mixture of SO_2 and oxygen, so the temperature profile is as follows:

$$\Delta_r G^{\varnothing} = 862.21 - 0.819 \cdot T, \quad \text{kJ} \cdot \text{mol}^{-1}, \quad \text{for } SO_2/O_2 \tag{33}$$

Equation (33) takes into account the reaction (31) (acc. [52]) and is consistent with the equation shown in [54]:

$$\Delta_r G^{\varnothing} = 98.60 - 0.094 \cdot T, \quad \text{kJ} \cdot \text{mol}^{-1}, \quad \text{for Equation (31)} \tag{34}$$

Equation (34) results from the difference of Equations (32) and (33) divided by the stoichiometric coefficient 3.

The kinetic data in Table 1 are quite divergent and relate to the decomposition reaction (30); the newer ones are numerically higher [56] and the older ones are lower [55]. In the first case, the analysis was carried out using thermogravimetry after isothermal dehydration in the temperature range of 823–923 K in air flow according to 0th order kinetics. In the second case, the process was carried out in a tubular reactor, isothermally with nitrogen flow, in the range 973–1123 K after dehydration removing gaseous products ($SO_3/SO_2/O_2$) from the reaction space, confirming the presence of SO_2 and oxygen. The study was conducted for an approximately spherical pellet of ferric sulphate for a kinetic model nowadays called the Jander model. The Arrhenius parameter pairs follow the KCE trend; these data determine $T_{eq} = 663.0$ K and this temperature was used further in the work. Further considerations were carried out for these two extremes of the kinetic data, shown in Figure 2a,b. Equilibrium temperature determined from Equations (32) and (33): $T_{eq} = 1052.81$ K, is indicated by line 1. Lines 1–4 follow the summary given in pt. 4.1, and line 2 determines ΔG^+ for numerically higher (Figure 2a) and lower (Figure 2b) kinetic data. The results of the catalyzed reaction (31) treating hematite as a catalyst, for a large excess flow of SO_3, were taken as the reversible reaction to (30). The activation process was considered to be revealed by the gas–solid surface contact. Line 5 follows from the Arrhenius equation according to [62] in the range $T = 1173 - 1323$ K:

$$k = 6.79 \times 10^5 \exp\left(-\frac{20{,}021}{T}\right), \quad \mathrm{s}^{-1} \tag{35}$$

used in Equation (12).

The temperature profile of the reaction (31) in the gas phase represented by Equation (34) is depicted by line 5, which for $T > T_{eq}$ is located between the temperature axis and line 1 (Figure 2b). Starting at $T > 1048$ K, the catalytic effect of hematite is practically identical to the equilibrium one determined by the conversion degree [63] which translates directly into the finding that line 5 is both a thermodynamic and kinetic description of the course of catalysis reaction (31) in the gas phase. Similar relationships between reaction rates and equilibrium relationships are expressed in work [55]. Thus, the equivalent to this reaction is line 4a shown in Figure 2. These are the activation states of the reaction (31) towards the hematite catalyst for higher (Figure 2a) and lower (Figure 2b) kinetic data; the latter are more in line with the considerations, as the surface activation of a specific volume is analyzed.

If we take T_{eq} as the temperature dividing the course of the reaction (30) into reversible and irreversible, the course of the reversible reaction analyzed for hematite as catalyst confirms that the course of the reaction in the gas phase is decisive (31). Thus, the three reactions: (30), (30) including (31) and (31) are characterized by a common isoequilibrium temperature since $\Delta_r G^{\varnothing} = 0$. Hematite as catalyst reproduces itself and does not convert to sulphate.

For the lower activation energy version, the temperature profiles 2 and 5 are mutually consistent, in particular as shown in Figure 2b. Line 5, after inversion of the signs and shifting upwards to the level of line 2 at equilibrium temperature, becomes a good illustration for consideration for option '0' (Equation (28)).

We searched according to Equation (18) for the activation equation for line 4b and the reaction (31) according to the linear relationship:

$$\Delta_{-1} G^+ = \Delta G^+ - \Delta_r G^{\varnothing} = 173.0 + 0.159 \cdot T \ \text{ for Equation (31)} \tag{36}$$

where ΔG^+ is provided in Table 1, and $\Delta_r G^{\varnothing}$ corresponds to Equation (34).

To facilitate considerations, it was assumed that lines 2 and 4b (on Figure 2b) constitute a common result set.

Coefficients of Equation (36) for the given four points are given in the caption under Figure 2 (line 4b) and are 155.46 kJ·mol^{-1} (intercept) and 0.154 kJ·mol^{-1}·K^{-1} (slope), respectively. The intercept differences are acceptable as minor.

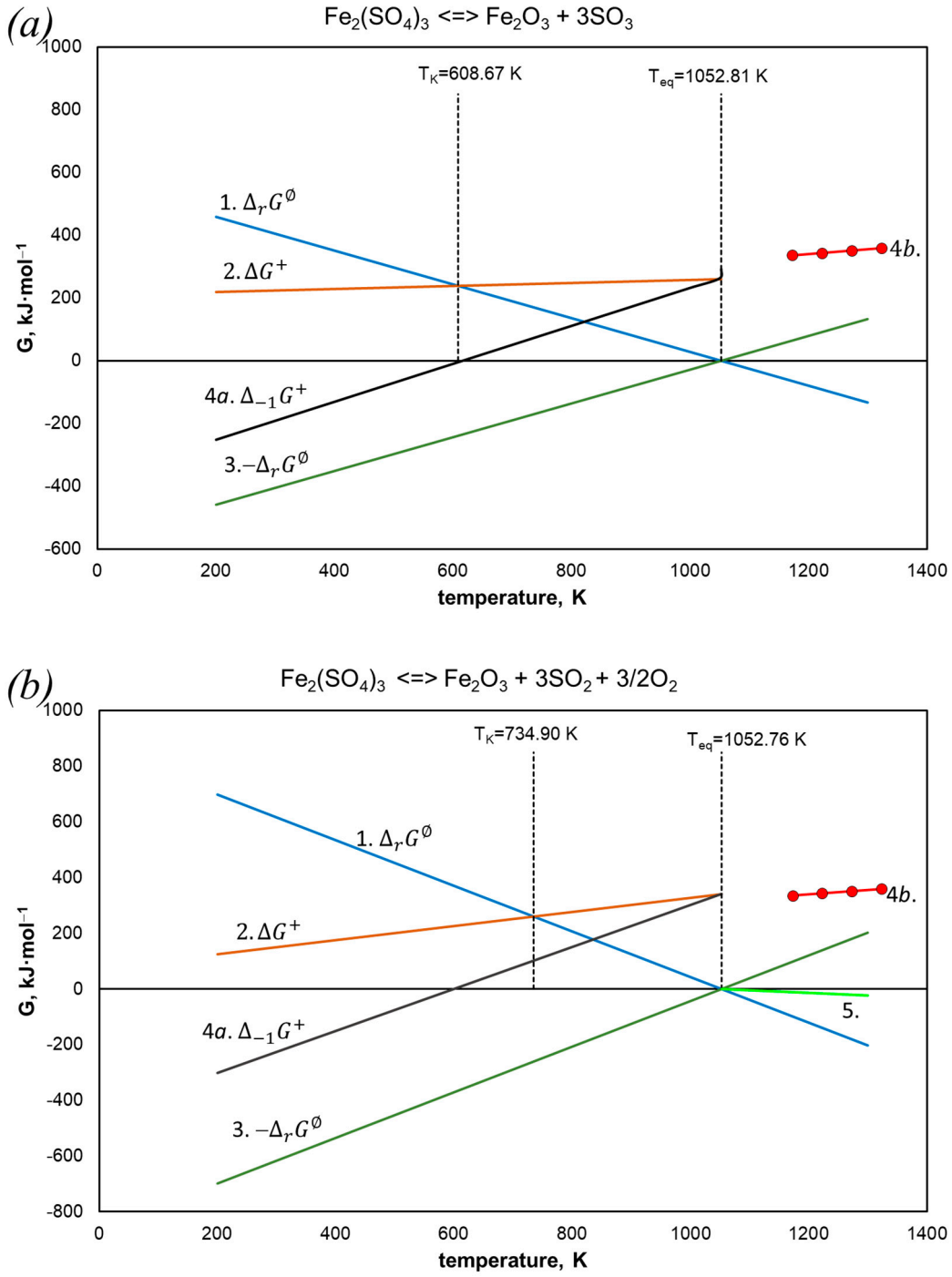


Figure 2. Temperature profiles for reactions (30), (30) with (31) and for (34) for: (**a**) 1. line acc. Equation (32), 2. Equation (11) for E = 218.4 kJ·mol^{-1}; ln A = 25.84 (A in s^{-1}), T_{eq} = 1052.81 K; T_K = 608.67 K, 3. line for a reversible reaction; sign inversion in Equation (32), 4a. $\Delta_{-1}G^{+} = -372.66 + 0.605 \cdot T$, 4b. for Equations (12) and (31) with Equation (35): $\Delta_{-1}G^{+}_{exp} = 155.46 + 0.154 \cdot T$, (**b**) 1. line acc. Equation (33), 2. Equation (11) for E = 83.3 kJ·mol^{-1}; ln A = 1.33 (A in s^{-1}), T_{eq} = 1052.76 K; T_K = 734.90 K, 3. line for a reversible reaction; sign inversion in Equation (33), 4a. $\Delta_{-1}G^{+} = -452.11 + 0.754 \cdot T$, 4b. as in (**a**), 5. Equation (34) for reaction (31)—only in (**b**).

The result of the calculations indicates the correctness of the concept, which makes it possible to independently analyze the catalytic process in the gas phase of activation reaction (31), consistent with the activation of thermal dissociation of the solid phase.

4.4. Aluminum Sulfate

As before, the fundamental problem that arises in the study is the thermal stability of SO_3. In the reaction record in Table 1, the gaseous product is SO_3:

$$Al_2(SO_4)_3{}^s \leftrightarrow \gamma\text{-}Al_2O_3{}^s + 3SO_3{}^g \quad (37)$$

The kinetic data of the parallel study to the previous one (ferric sulfate) described in [55] are for the study in a nitrogen atmosphere, in which, as before, the resulting gases ($SO_3/SO_2/O_2$) were derived from the reaction zone. Figure 3 shows the temperature profiles of the reaction (37).

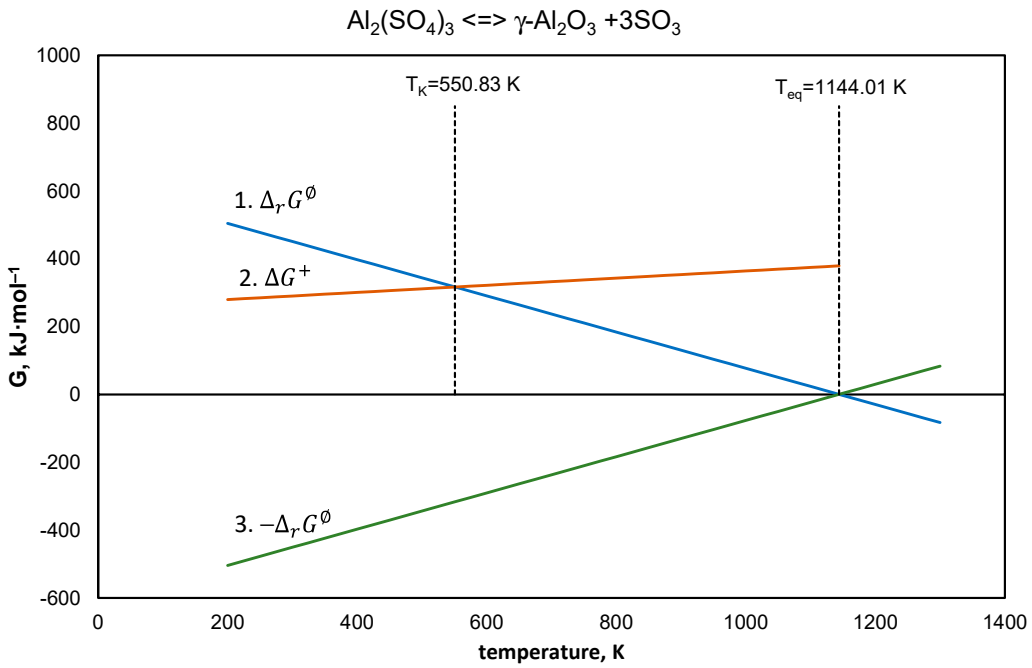


Figure 3. Thermodynamic analysis of the reaction (37) course. Only lines 1–3 are marked, T_{eq} = 1144.01 K, T_K = 550.83 K; line 2 follows from Table 1.

In this case, it is not possible to analyze a reaction reversible to (36), since Al_2O_3 (in a mixture with SiO_2) is inert towards SO_3 [61]. The only evidence to recognize the validity of the TST for the reaction (37) is the fact of the appropriate choice of kinetic data, since the existence of the isoequilibrium temperature determines the equilibrium activation constant K^+, which is an infinitesimally small quantity.

4.5. Silver Nitrate

In Table 1 the following reaction is considered:

$$2AgNO_3{}^s \leftrightarrow 2Ag^s + O_2{}^g + 2NO_2{}^g \quad (38)$$

but for thermodynamic and kinetic analyses, the equations were related to 1 mole of $AgNO_3$.

The decomposition of $AgNO_3$ may occur through the formation of silver oxide and its decomposition in the reaction mechanism [57]:

$$Ag_2O^s \rightarrow 2Ag^s + 1/2\ O_2{}^g \quad (39)$$

and ultimately:

$$2NO_2{}^g \rightarrow 2NO^g + O_2{}^g \quad (40)$$

In the light of these possibilities, the reversible reaction to (38) implies the formation of $AgNO_3$ from gaseous reactants and metallic silver:

$$Ag + NO_2 + 1/2O_2 \text{ or } Ag + NO + O_2 \rightarrow AgNO_3 \quad (41)$$

Practical demonstration of the reaction (41) course is not straightforward due to silver's passivity towards complex mixtures of nitrogen and oxygen oxides. The basic properties of $AgNO_3$ are as follows [64]: melting point 212 °C (485 K), thermal decomposition 250–440 °C (523–713 K), metallic silver appears with the onset of boiling above 440 °C (713 K), determined at 422.74 °C (695.89 K), and total decomposition of 'intermediary compounds' (probably metal oxide [57]): above 608 °C (881 K).

Figure 4 shows the temperature profiles for the data presented in Table 1 and reaction (38), which translates into metallic silver as the final product, but $T_{eq} = 649.25$ K is lower than for the total decomposition to free metal.

It provides another opportunity to write the reaction:

$$2\ AgNO_3{}^{s} \rightarrow Ag_2O^{s} + 2NO_2{}^{g} + 1/2O_2{}^{g} \quad (42)$$

in the temperature range up to $T = 600$ K [52], we obtain the relationship:

$$\Delta_r G^{\varnothing} = 137.62 - 0.199 \cdot T, \quad \text{kJ} \cdot \text{mol}^{-1}, \quad \text{for Equation } (42) \quad (43)$$

from which $T_{eq} = 691.56$ K and it is practically consistent with experience, but is higher than that resulting from the total decomposition reaction to the free metal (38).

From an extensively reviewed thermogravimetric study of the thermal dissociation of commercial silver nitrate (in an argon atmosphere), the parameters of the Arrhenius equation given in Table 1 were recognized. They are the result of the averaging procedures described in [57] and agreement with these considerations is shown by Equation (27) in analytical form:

$$\Delta G^{+} = 124.94 + 0.132 \cdot T, \quad \text{kJ} \cdot \text{mol}^{-1} \quad (44)$$

The corresponding constants of Equation (44) according to work [57] are: 138.7 $\text{kJ} \cdot \text{mol}^{-1}$ and 0.12 $\text{kJ} \cdot \text{mol}^{-1} \cdot \text{K}^{-1}$. The differences are due to the different way of determining the Arrhenius equation parameters and the adopted scale of characteristic temperatures.

It is puzzling whether on Figure 4 in light of these properties it is correct to assume metallic silver or its oxide as the products of the irreversible reaction. After all, complete decomposition (with separation of metallic silver) occurs above T_{eq} = 649.3–691.5 K, which should logically point to 'intermediary compounds' (Ag_2O) as the transition state [57]. According to the principles of phenomenological thermodynamics, we assume a temperature range for the reactions leading to the final solid phase products. It is theorized that a reversible reaction proceeds to full decomposition in the temperature interval for the condition of $\Delta_r G^{\varnothing} = 0$.

Thus, the analysis presented here demonstrates the acceptability of TST for reaction studies (42) despite the complexity of homogeneous reactions in the gas phase. Puzzlingly, the low isoequilibrium temperature ($T_K = 84.53$ K) suggests that the kinetic parameters are too far from the expected ones, which is somehow limited by the temperature profile of the reversible reaction for Equation (44).

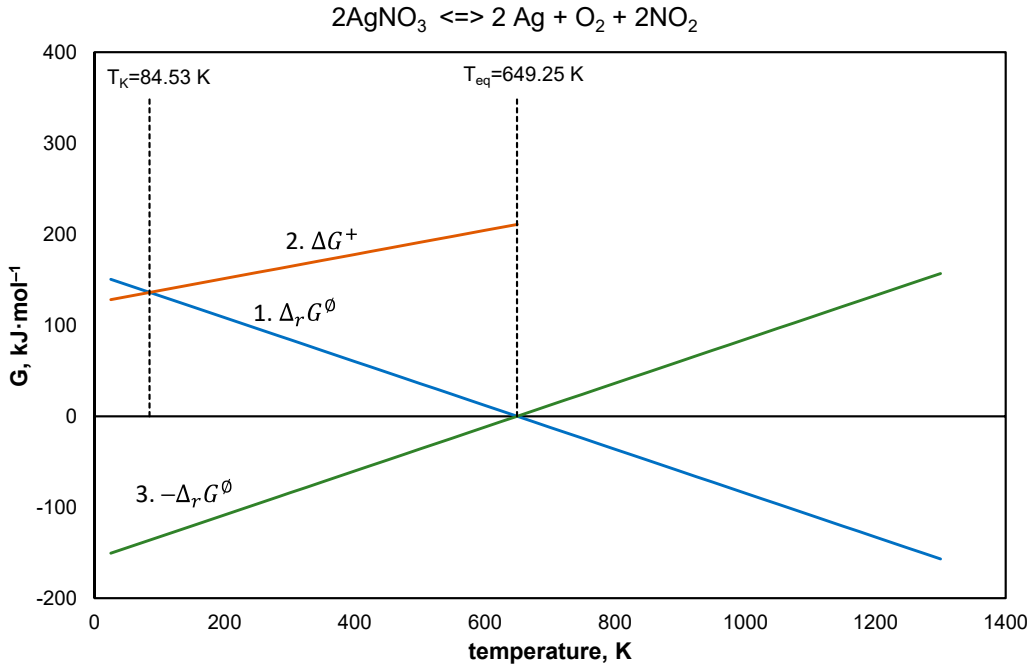


Figure 4. Temperature profiles for the reaction (38), lines 1–3 are marked, T_{eq} = 649.25 K, T_K = 84.53 K; line 1. according to Equation (26) and the data given in Table 1, line 2. expresses Equation (44), line 3. is formed by inversion of the signs of line 1.

4.6. Ammonium Perchlorate

Table 1 shows the course of the decomposition reaction for the two versions:

$$4NH_4ClO_4{}^s \rightarrow 4HCl^g + 2N_2{}^g + 5O_2{}^g + 6H_2O^g \quad (45)$$

$$2NH_4ClO_4{}^s \rightarrow Cl_2{}^g + N_2{}^g + 2O_2{}^g + 4H_2O^g \quad (46)$$

in which only gaseous products are obtained from solid ammonium perchlorate in an exothermic decomposition reaction.

It should be noted that the thermodynamic data for $\Delta_r G^{\varnothing}$ capture the aforementioned two equations, ignoring other known decomposition possibilities [65], while for activation they capture only one pair of kinetic parameters for the full solid-phase decomposition acc. Anderson (set 7 and 8 in [53]) for dynamic and isothermal conditions.

Analyzing the reactions (45) and (46), their irreversibility can be recognized a priori, as confirmed by the relevant relations $\Delta_r G^{\varnothing} < 0$ and $\Delta G^+ > 0$ (Table 1, Figure 5). Figure 5 shows the relevant relations mentioned in the figure caption.

The situation analyzed provides a formal opportunity to assess the indiscriminate application of kinetic data to TST. For this purpose, the approach acc. Equation (12) is most favorable while:

$$k \leq \mathrm{B}T, \quad \text{then} \quad \Delta G^+ \geq 0 \quad (47)$$

At a temperature of T = 500 K, acc. Equation (47) for $\Delta G^+ = 0$, $k = 1.042 \times 10^{13}$ s^{-1}, and for the analyzed case is $k = 2.57$ s^{-1} (for calcite at this temperature $k = 5.42 \times 10^{-14}$ s^{-1}) and so this is a fast reaction in the slow reaction category. Note that Figure 5 shows the negligible influence of the ΔG^+ profiles (lines 2) relative to the $\Delta_r G^{\varnothing} \ll 0$ thermodynamic profiles (lines 1). The postulate written by inequalities (47) concerns the kinetics of reactions after initiation that proceed spontaneously ($K \rightarrow \infty$). It is therefore rare in the analysis of chemical compounds, as it represents a thermal dissociation process with an exothermic effect.

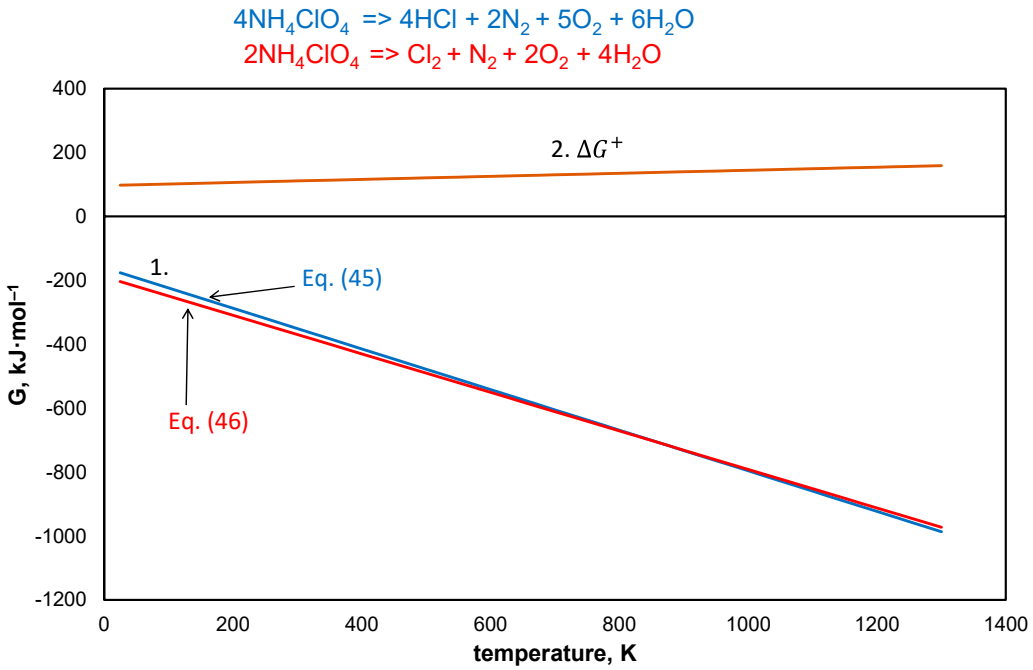


Figure 5. Temperature profiles of reactions. Lines 1. for $\Delta_r G^{\varnothing} = -159.98–0.636\ T$ and $\Delta_r G^{\varnothing} = -188.78–0.603\ T$, line 2. for both versions $\Delta G^{+} = 96.83 + 0.048 \cdot T$.

5. Entropy of Activation at Isokinetic Temperature

An analysis of Equation (1) by comparing the temperature profiles according to the Gibbs free energy (Equation (26)) and the activation energy according to Equation (27) was proposed. In this work, temperature profile means an analytical relation valid for a specific temperature range and used in any scope. The reactants selected for analysis are summarized in Table 1, assigning the appropriate equations, and commentary and Figures 1–5 in the text. Lines 1 denote directly Equation (26) from which the equilibrium temperature from the relation $\Delta_r G^{\varnothing} = 0$. Lines 2, on the other hand, are an approximation according to Equation (27) and arise from the implementation of the Arrhenius parameters according to TST. Lines 3 are reversible reactions whose slope indicates the direction of the reaction for the constraint $\Delta_r G^{\varnothing} \leq 0$.

In the light of the examples presented, new problems still emerge as to how the Gibbs free energy equations of the activation state (Equations (11) and (12)) are related to the reversible reaction (line 3), and isoequilibrium and isokinetic temperatures.

The notation of Equation (18) follows directly from the arguments presented in paper [19] and more recent ones [27,34]. The term $\Delta_{-1} G^{+}$ is related to the activation of the reversible reaction in Equation (12) for the reaction rate constant $k_{-1.}$

Another important element is the isoequilibrium temperature, which results from the comparison of lines 1 and 2 (which has been assigned the subscript K or $-K$ as opposed to the frequently used subscripts *iso* or *c*) and the attribution of its stated meaning is as suggested by Krug [66]. This is presented by Equation (22) and for a reversible reaction/process by Equation (23).

The existence of an isoequilibrium temperature is indicative of the kinetic nature of the reaction; within the framework of reactions described as slow, a distinction should also be made between definitely slow. This can either be a characteristic of the reaction or clearly higher than appropriate parameters according to Arrhenius' law.

The approach acc. Equation (18) on the left-hand side ties together the relationships of phenomenological thermodynamics with the difference on the right-hand side of the activation thermodynamic terms determined from kinetic studies. While in the analyzed temperature ranges the thermodynamic expression is invariant (constant), the right-hand

side is dependent on the kinetics, which can be described by many models, especially those satisfying KCE.

The last element that is generally known from the literature is the KCE. This means that the Arrhenius kinetic parameters satisfy a linear relationship of the common direction of increasing (or decreasing) change. For this purpose, Equation (11) is presented as:

$$\Delta G^{+} = E - \mathrm{R}T\ln A + \mathrm{R}T\ln(\mathrm{B}T) \tag{48}$$

and then for the first two terms of the right side of Equation (48) KCE was entered and for $T = T_{iso}$ we obtain Equation (12) in form:

$$\Delta G^{+}(T_{iso}) = \mathrm{R}T_{iso}\ln\left(\frac{\mathrm{B}T_{iso}}{k_{iso}}\right) = \text{const} \tag{49}$$

or after writing:

$$\Delta G^{+}(T_{iso}) = E + \mathrm{R}T_{iso}\ln\left(\frac{\mathrm{B}T_{iso}}{A}\right) = \text{const} \tag{50}$$

In particular, Equation (49) indicates that T_{iso} is also the isoequilibrium temperature but only for activation states.

To determine the entropy at isokinetic temperature, Equation (14) can be used; it is more preferable to insert Equation (49) into Equation (13).

After ordering, we obtain:

$$\Delta S^{+} = \frac{\Delta H^{+}}{T_{iso}} + \mathrm{R}\ln\left(\frac{k_{iso}}{\mathrm{B}T_{iso}}\right) \neq \text{const} \tag{51}$$

and from Equation (14):

$$\Delta S^{+} = \mathrm{R}\left[\ln\left(\frac{A}{\mathrm{B}T_{iso}}\right) - 1\right] \neq \text{const} \tag{52}$$

According to Equation (51), the activation entropy at isokinetic temperature depends on $\Delta H^{+}(= E - \mathrm{R}T_{iso})$ and according to Equation (52) on $\ln A$., Equation (51) is interesting for following a group of reactions in the liquid phase (formation of metalloporphyrins at assumed temperature 298 K = const [42]).

Conner [18] established the relationship between activation entropy and activation energy, while [27] proposed Equation (53) in the form of a notation later named after him as the Yelon Equation (34):

$$\Delta S^{+} = \frac{\Delta H^{+}}{T_{iso}} + \Delta S_B \tag{53}$$

where:

$$\Delta S_B = \mathrm{R}\ln\left(\frac{k_{iso}}{\mathrm{B}T_{iso}}\right) = \text{const} \tag{54}$$

Equation (53) is another form of notation of EEC versus isokinetic temperature T_{iso}.

The activation entropy expressed in Equation (54) was defined as Multi-Excitation Entropy [27] and it disappears when we create differences according to Equation (53), and also according to Equation (51) for two pairs of Arrhenius parameters:

$$\Delta\left(\Delta S^{+}\right) = \frac{|\Delta E|}{T_{iso}}, \quad T_{iso} = \text{const} \tag{55}$$

or again using KCE:

$$\Delta\left(\Delta S^{+}\right) = \mathrm{R}|\Delta\ln A|, \quad T_{iso} = \text{const} \tag{56}$$

Equation (56) is a notation of differences acc. Equation (52) for the next two values of pre-exponential factor A.

For isoconversional methods, when the parameters of Arrhenius' law change with conversion degree ($E = E(\alpha)$), then Equation (56) is the simplest tool for stepwise analysis, as long as the data meet KCE (Appendix A.2).

In Equations (55) and (56), the order of accepted nodes is not imposed, so the sign will depend on the accepted order of operations. For these reasons, we accept the presented notation as absolute values.

The geometric interpretation of Equations (55) and (56) is presented in Figure 6, which, as suggested by [67], shows the identity of the isokinetic/compensatory temperature for KCE/EEC, thanks to the constancy of activation entropy changes at this temperature. These equations can be used both for 'step by step' data and extrapolating for kinetics when $E = 0$, $A = k_{iso}$.

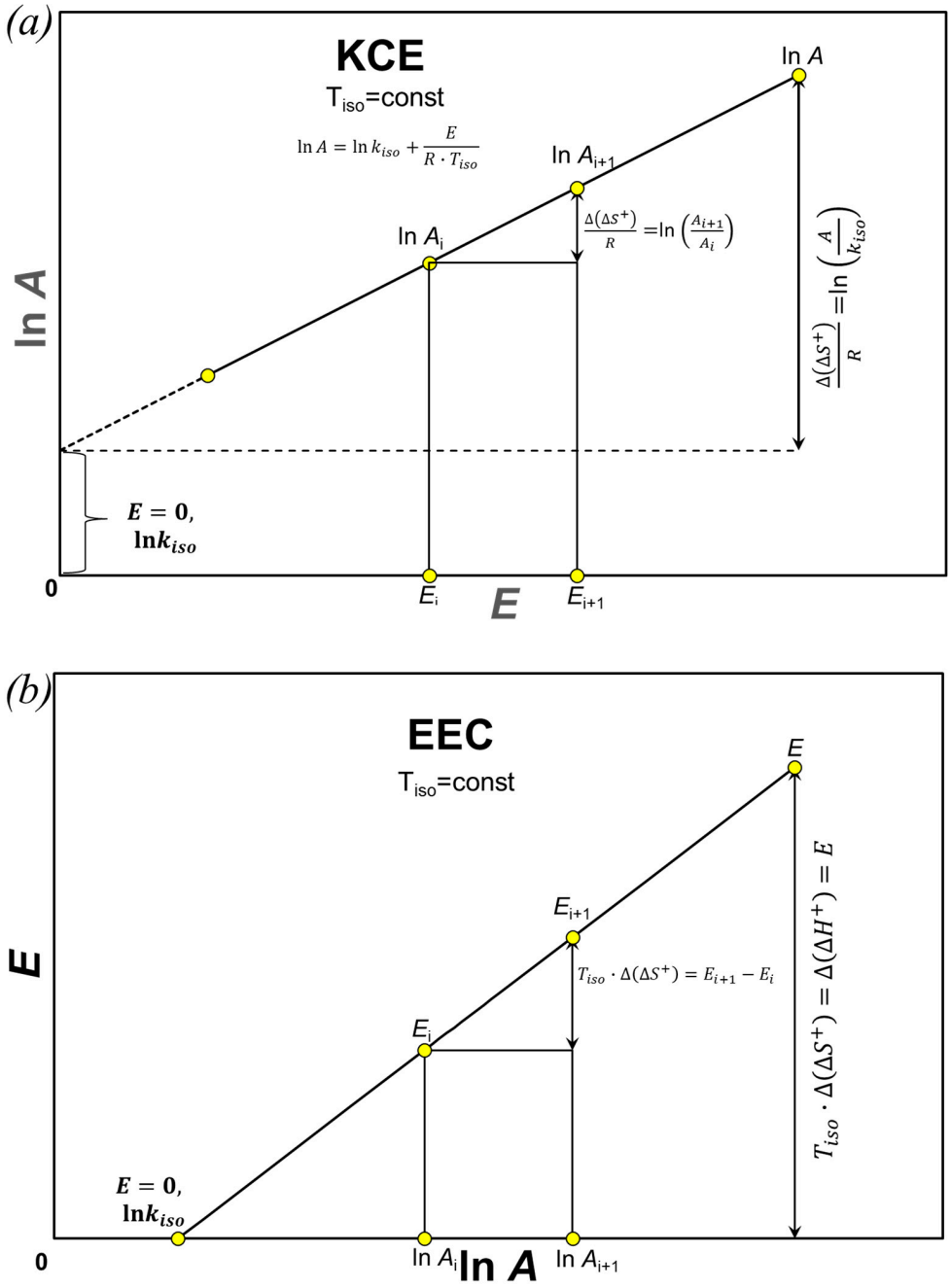


Figure 6. KCE plot including activation entropy at isokinetic temperature; (**a**) classic approach; (**b**) KCE after changing variables is transformed into EEC.

Using Equation (50) for the isokinetic temperature T_{iso} = 663.0 K previously determined for ferric sulfate and two pairs of Arrhenius parameters presented in Table 1 (E = 218.4 kJ·mol^{-1}; ln A = 25.84—Figure 2a and E = 83.3 kJ·mol^{-1}; ln A = 1.33 —Figure 2b), we obtain the same result in both cases ($\Delta G^{+}(T_{iso})$ = 242.70 kJ·mol^{-1}). According to Equation (54) we get ΔS_B = −366.1 J·mol^{-1}·K^{-1}), and according to Equations (55) and (56) $\Delta(\Delta S^{+})$ = 203.8 J·mol^{-1}·K^{-1}, which at the same time constitutes the activation entropy for the transition of two different kinetic characteristics satisfying KCE.

The validity of the calculations is confirmed by EEC by determining the difference here defined by the symbol $\Delta(\Delta S^{+}) = |\Delta a_3| = |0.253 - 0.048| = 0.205 \times 10^3$ J·mol^{-1}·K^{-1}, where the activation entropies used were taken from Table 1. KCE is represented by the isokinetic temperature, which is also isoequilibrium one since $\Delta G^{+}(T_{iso})$ = const. It generally remains lower than the equilibrium temperature T_{eq} [63], but higher than the isoequilibrium temperature T_K when $\Delta_r G^{\varnothing} = \Delta G^{+}$ (Equation (22)).

Much attention has been paid to the issue of KCE. Recently, a new criterion for assessing the reliability of the experimentally determined isokinetic temperature was proposed [68,69], which was used in another work [70]. The value determined in this work is only an illustrative quantity (from two points), but it sufficiently creates the significance of the KCE by analyzing changes in the activation entropy depending on the isokinetic temperature.

KCE understood as the linear relationship $\ln A \propto \frac{E}{RT_{iso}}$ indicates the influence of isokinetic temperature on the isoequilibrium temperature. If the isokinetic temperature tends towards very high values ($T_{iso} \to \infty$), the more $T_K \to 0$, and thus the chronicity of the decomposition reaction is confirmed.

Of the five examples considered, if we accept the verifications according to Equations (11), (12) and (18), with Equation (28) as zero option, then in each case there is a premise to reject only the thermal decomposition of ammonium perchlorate according to TST.

6. Discussion

Equation (3) is the most commonly used form of TST, which omits complex considerations of the partition functions of the reactant and the activated complex, and thus does not take into account the motion over the saddle point [71]. This equation is presented in the simplest form (apart from the temperature) with a single frequency variable ν:

$$k_{TST} = \chi \cdot \frac{\nu}{1 - \exp\left(-\frac{\nu}{BT}\right)} \cdot \exp\left(-\frac{\Delta G^{+}}{RT}\right) \tag{57}$$

For $\nu \gg BT$, Equation (57) is simplified to the form [19]:

$$k_{TST} = \chi \cdot \nu \cdot \exp\left(-\frac{\Delta G^{+}}{RT}\right) \tag{58}$$

and to expand the expression in the denominator of Equation (57) for $\nu \ll BT$ into a series and stop at the first two expressions, the form of Equation (3) is obtained.

Using the concept of vibration frequency in Equations (57) and (58), we can refer to the transmission coefficient. Typically, its value is taken as $\chi = 1$, but in the interactions of two reactants the coefficient $\chi \gg 1$ [46]. It depends on the size of the reactive surface [41].

In accordance with the views presented in [25,26,72], one most reasonable equation was adopted for the considered reactions with the following mathematical structure, in which ν denotes the decomposition frequency of transition state [30]:

$$\chi = 1 + \frac{1}{24}\left(\frac{\nu}{BT}\right)^2 \tag{59}$$

Based on [36,72]:

$$\nu = \mathrm{B}T_{iso} \tag{60}$$

and finally:

$$\chi = 1 + \frac{1}{24}\left(\frac{T_{iso}}{T}\right)^2, \text{ where } T > T_{iso} \tag{61}$$

but for $T = T_{iso}$, $\chi = 1.042$.

For example, for calcite and simplex of the isokinetic temperature ($T_{iso} = 914.29$ K [73]) to the equilibrium temperature ($T_{eq} = 1166.13$ K), $\chi = 1.026$. According to Equation (61) and for the archival data according to [74], assuming the inverse (literally) of 'natural period of oscillation of the atom of the substance', $\nu = 7.25 \times 10^{12}$ s^{-1} ($\nu = 10^{13}$ s^{-1}) [75] then at the equilibrium temperature $\chi = 1.004$ ($\chi = 1.007$).

Very often the inequality $T_{iso} > T_{eq}$ is characteristic for isoconversion methods, so this temperature should be approached with caution [76] and T_{iso} is considered equivalent to TST due to the activation entropy in the notation of Equation (53). To the expression $1/T_{iso}$ is assigned a measure of deviation from detailed equilibrium [36]. According to the concept of [73], theoretically $T_{iso} \to T_{eq}$.

Lyon [77] assumed that for dynamic conditions the isokinetic temperature T_{iso} is also the equilibrium temperature T_{eq}, i.e., according to Equation (16), $T_{iso} \to \frac{\Delta_r H^{\varnothing}}{\Delta_r S^{\varnothing}}$, which can be considered an approximation extremely useful for practice, usually $T_{iso} \neq T_{eq}$.

7. Final Remarks

Šimon is very careful about the sense of determining activation parameters in each case, because 'what is the structure of the activated complex in case of complex processes?' [78]. In turn, Khrapunow [32] believes that according to known methods of determination, the activation enthalpy can be accepted, but the entropy is controversial. In their book publications, Vyazovkin [79] discusses the Lumry–Eyring law, while Šesták [80] devotes more attention to the discussion related to the Arrhenius vs. non-Arrhenius relationship than to the Eyring equation. Against the background of these books and issues in terms of [29,30,78,81], the issue of TST is an extremely important issue in relation to the classical Arrhenius equation, at the same time emphasizing the aspect of modernity. Nevertheless, against the background of the cited considerations, this work seems to be justified, although it in no way solves the doubts related to TST. However, attention was paid to several new elements in the considered issue.

In this state of partial problems, TST certainly cannot be applied to complex systems, in particular biomass decomposition, as well as an inherently complicated issue arises, which is the validity of the Arrhenius law parameters, in particular correlated as KCE. The lack of reversibility of the reaction makes it impossible to refer to the determined entropy, which depends on the way of interpreting its nature (Multi-Excitation Entropy [27]) or its anthropomorphic nature. That is, in other words, its ultimate dependence on the task posed [82]. An example following these considerations are Equations (51), (55) and (56); in this case, the common point is the isokinetic temperature T_{iso}.

8. Proof of Concept

It was assumed that for the adaptation of selected TST elements for solid-phase thermal dissociation understood in terms of chemically defined compounds, the basic condition is the reversibility of the chemical reaction, possibly associated with a catalytic process. It proceeds with the transition state of the active structure. The formal notation of Equation (1) combines phenomenological thermodynamics with kinetic constants that describe the thermodynamics of the activation process captured by Equation (18).

Knowledge of two of the three components provides the possibility of verifying the full cycle of the reaction/process run by looking for the third component or directly by accepting the TST for the 'forwards to backwards' run, which leads to an extension of the

interpretative possibilities to the thermodynamics of activation. The cycle analysis requires knowledge of the equilibrium temperature T_{eq} (Equation (16)).

In the provided examples, the postulate about the linearity of Gibbs free enthalpy ($\Delta_r G^{\varnothing}$) and free enthalpy of activation (ΔG^{+} and next) vs. temperature proved to be correct. For example, of interest is the low temperature (26–43 °C) membrane fusion reaction/process, when ΔG^{+} is 3rd degree polynomial with a tendency to decrease with temperature [83].

In the cases considered here, we observe the opposite situation, i.e., a positive increase in ΔG^{+} with increasing temperature up to the T_{eq} limit. In other words, this implies an increasingly difficult activation process which, with decreasing temperature, leads to the activation of a reversible reaction. $\Delta G^{+} > 0$ is dependent on kinetic qualities, primarily the negative entropy of activation, which occurs when the thermodynamic stimulus $\frac{k_B}{h} T > k$ (Equation (12)). The simplest explanation of these observations is illustrated by the 'zero option' captured by an approximation that is close to model considerations (Equation (28)).

The temperature profiles of free enthalpy of activation straight line ΔG^{+} intersecting with straight line $\Delta_r G^{\varnothing}$, determine isoequilibrium temperature (T_K, Equation (22)), which further confirms the possibility of using the TST, as we can determine the equilibrium constant of activation (Equation (25)).

The choice of kinetic parameters according to Arrhenius remains a completely different issue; in this work it is tacitly assumed that these quantities remain authoritative with respect to the TST. Very often, however, they are derived from microscale thermogravimetric studies under dynamic conditions, and the kinetic parameters are determined by isoconversion methods. Undoubtedly, this problem requires further consideration and in this respect it is certainly more reasonable in the TST formulae to adopt an isokinetic temperature (T_{iso}), which is close to the equilibrium temperature (T_{eq}), in place of the temperature of the maximum reaction rate (T_m). The latter is in fact characteristic only of dynamic conditions. However, it is more correct to determine thermodynamic activation functions at temperatures for which $E = E(\alpha)$ has been determined.

A synthetic summary of the analyses leads to the conclusion that the TST extends the possibilities of interpretation of thermal dissociation of solid chemical substances, occurring in relation to Equation (1) when reduced to a description of the thermodynamics of the activation process included in Equation (18), which connects phenomenological thermodynamics with activation. An additional value strengthening the postulate is the existence of isoequilibrium temperature (Equations (22) and (25)).

9. Conclusions

Numbering of straight lines is consistent with the entry in sub-point 4.1.

1. The reference to the thermodynamic equilibrium constant in terms of the kinetic dissociation reaction/process of solids to its reversibility (Equation (1)) creates the possibility of identifying the thermodynamics of activation processes according to TST. The possibility of analyzing 'forwards to backwards' relations for these issues is therefore extended, which is made possible by the relational Equation (18).
2. This temperature is common to the activation process of thermal dissociation and reversible synthesis. The isoequilibrium temperature (T_K) is of great importance and is determined by the intersection of the Gibbs free energy (lines 1 and 2), i.e., according to the thermodynamic approach and determined by the kinetic parameters of this distribution for the reversible reaction.
3. The crux of the matter leads to the equality of the equilibrium constants for the decomposition reaction and those experimentally determined for the reversible reaction.
4. Therefore, it is extremely important to correctly determine Arrhenius kinetic parameters. KCE is based on isentropic equilibration of these parameters at isoconversion temperature T_{iso} close to equilibrium temperature T_{eq}.

Author Contributions: Conceptualization, A.M. and T.R.; methodology, A.M.; validation, A.M., T.R. and R.B.; formal analysis, A.M. and T.R.; investigation, A.M.; resources, T.R.; data curation, A.M.; writing—original draft preparation, A.M. and T.R.; writing—review and editing, R.B. and T.R.; visualization, T.R.; supervision, A.M.; project administration, A.M. and R.B. All authors have read and agreed to the published version of the manuscript.

Funding: This research received no external funding.

Data Availability Statement: Data are contained within the article.

Conflicts of Interest: The authors declare no conflict of interest.

Nomenclature

a_0 , a_1, a_2, a_3	coefficients of strictly thermodynamic significance
A	pre-exponential factor, s^{-1}
B	$2.08364 \cdot 10^{10}$ $K^{-1} \cdot s^{-1}$ ratio of Boltzmann to Planck's constant
C	const in Equation (28), $J \cdot mol^{-1}$
E	activation energy, $J \cdot mol^{-1}$
ΔG, ΔH, ΔS and G, H, S	thermodynamic functions; respectively: free enthalpy, enthalpy, and entropy
$\Delta_{-1}G^{+}$	temperature profile of a reversible reaction, $J \cdot mol^{-1}$
ΔS_B	activation entropy in isokinetic temperature (Multi-Excitation Entropy) Equations (53) and (54), $J \cdot mol^{-1} \cdot K^{-1}$
h	$6.62607 \cdot 10^{-34}$ J·s, Planck constant
k	rate constant, s^{-1}
k_B	$1.38065 \cdot 10^{-24}$ $J \cdot K^{-1}$, Boltzmann constant,
K	equilibrium constant
n	0, 1, or 2, coefficients
P	pressure, MPa
R	8.314 $J \cdot mol^{-1} \cdot K^{-1}$, universal gas constant
r^2	coefficients of linear determination
q	heating rate, $K \cdot s^{-1}$
t	time, s
T	absolute temperature, K
α	conversion degree, $0 < \alpha \leq 1$
χ	transmission coefficient
ν	frequency (decomposition frequency of transition state [25]) s^{-1}
Subscripts	
0	initial
1,2	forward
-1	backward
c	compensation
eq	equilibrium
exp	experiment
f	final
i	i^{th} value
iso	isokinetic value
K	isoequilibrium for forward
$(-K)$	isoequilibrium for backward
m	maximum of rate reaction/process
r	reaction
TST	Transition-State Theory
Superscripts	
+	activation functions
$\varnothing$	standard condition
g, s	gas, solid

Abbreviations

FWO	Flynn–Wall–Ozawa Equation,
KAS	Kissinger–Akahira–Sunose Equation,
EEC	Entalphy–Entropy Compensation,
KCE	Kinetic Compensation Effect (IE or Constable plot, also IKR),
RPM	Random Pore Models [58],
RRKM	Rice–Ramsperger–Kassel–Marcus Theory [51],
TST	Transition-State Theory.

Appendix A

Appendix A.1. General form of Equations (22) and (23)

According to the finding that all ΔG relationships are linearly dependent on T, then acc. Equations (26) and (27), Equation (22) can be written as:

$$\Delta_r G^{\varnothing} = m\Delta G^{+} + p, \quad \text{where : } m\,, p\text{—coefficients} \tag{A1}$$

and acc. Equation (18) the following relationship is valid:

$$\Delta_{-1} G^{+} = (1 - m)\Delta G^{+} - p \tag{A2}$$

According to Equation (19) $\Delta G^{+}(T_{eq}) = \Delta_{-1} G^{+}(T_{eq})$ and acc. Equation (22) $\Delta_r G^{\varnothing}(T_K) = \Delta G^{+}(T_K)$ and after elimination of constants once determined, we obtain:

$$\Delta_r G^{\varnothing} = \Delta G^{+}(T_K)\frac{\Delta G^{+}(T_{eq}) - \Delta G^{+}}{\Delta G^{+}(T_{eq}) - \Delta G^{+}(T_K)} \tag{A3}$$

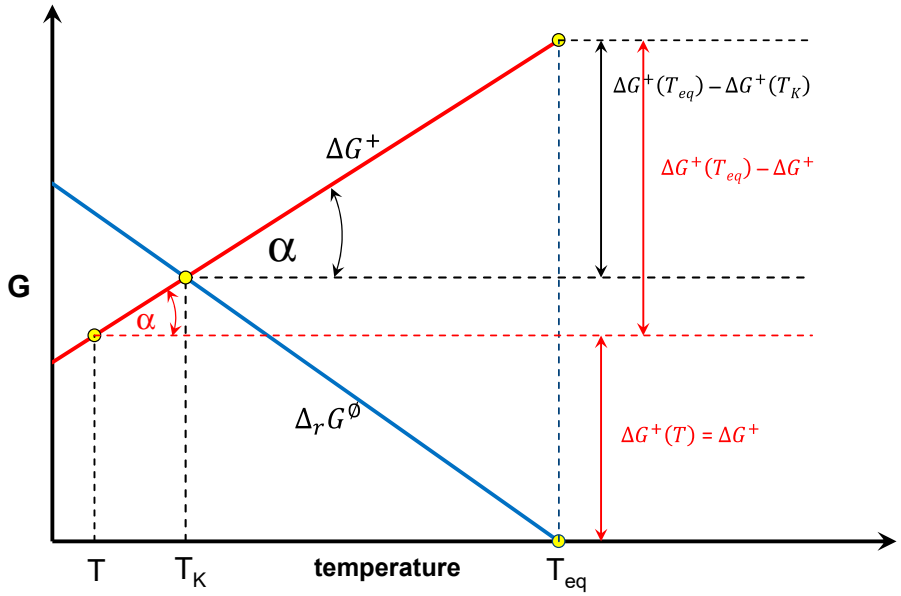


Figure A1. Chart of temperature profiles linking $\Delta_r G^{\varnothing}$ to the activation process ΔG^{+} Yellow points indicate characteristic temperatures. Blue line—line 1 acc. Equation (26), red line—line 2 acc. Equation (27).

From the comparison of the slope of ΔG^{+} vs. T (tg α) we finally obtain the expression Equation (A3) on a proportional basis:

$$\Delta_r G^{\varnothing} = \Delta G^{+}(T_K)\frac{T_{eq} - T}{T_{eq} - T_K} \tag{A4}$$

For $T = T_K$, $\Delta_r G^{\varnothing} = \Delta G^{+}(T_K)$, Equation (22), and for $T = T_{eq}$, $\Delta_r G^{\varnothing} = 0$, Equation (16).

Equation (A4) is an extension of Equation (22) for any temperature $T > 0$. By substituting T_{-K} in Equation (A4) instead of T_K, we also obtain an extension of the interpretative possibilities for Equation (23).

Appendix A.2. Importance of Equation (14) in Relation to KCE Expressed by Equations (55) and (56)

In isothermal conditions, the application of Equation (14) is obvious, while dynamic conditions require some clarifications, assuming that we accept TST for the considered reaction/process.

In the interpretation of reactions/processes occurring in the condensed phase, Vyazovkin et al. [35,50] believe that there is a very strong connection between the activation entropy and the kinetics, represented by the pre-exponential Arrhenius constant, and to a lesser extent with the temperature. Equation (14) can be expressed as follows:

$$\Delta S^{+} = R{\cdot}\ln A - \mathrm{R}{\cdot}\ln T - \mathrm{const} \tag{A5}$$

which for $T = \mathrm{const}$ a linear relationship is observed ΔS^{+} vs. $\ln A$.

For dynamic conditions, i.e., linear temperature increase, the temperature of the maximum reaction/process rate is assumed as a constant value. This is only true when the heating rate is constant. But as the heating rate increases, the temperature of the maximum reaction rate shifts towards higher and higher values, which is captured by the Kissinger equation [17]. For complex thermal decompositions of selected phosphates, one heating rate was selected for calculations [84–86]. However, there are no precise provisions on how to choose the reference temperature; a clue may be the assumption that the approximate isokinetic temperature should be determined as the harmonic mean from the range of temperatures used [68].

According to the considerations of this work, in Equation (14), the isokinetic/compensatory temperature is the most justified quantity, because such an approach leads to KCE through partial relations Equations (55) and (56). The quoted equations still make a difference for two temperatures subscripted as j and i:

$$\Delta\left(\Delta S^{+}\right) = \Delta S^{+}\left(T_j \to T_i\right), \qquad T_j > T_i \tag{A6}$$

1. For T_{iso} (Figure A2a, points $1 \to 2$):

$$\Delta S^{+}\left(T_j \to T_i\right) = \mathrm{Rln}\,\frac{A_j}{A_i} \tag{A7}$$

2 For $\alpha = \mathrm{const}$, $q = \mathrm{var}$ (Figure A2a, points $3 \to 4$, from Equation (A5)):

$$\Delta S^{+}\left(T_j \to T_i\right) = \mathrm{R}\left(\ln\frac{A_j}{A_i} - \ln\frac{T_j}{T_i}\right) \tag{A8}$$

3 For $\alpha = \mathrm{var}$, $q = \mathrm{const}$ (Figure A2b):

$$\Delta S^{+}\left(T_0 \to T_f\right) = -\mathrm{Rln}\,\frac{T_f}{T_0} < 0 \tag{A9}$$

When the numerical value of the term $\left|\mathrm{Rln}\,\frac{\mathrm{T_j}}{\mathrm{T_i}}\right|$ is much smaller than $\left|\mathrm{Rln}\,\frac{\mathrm{A_j}}{\mathrm{A_i}}\right|$, then the temperature ratio becomes less and less important.

For example, for calcite in isothermal conditions we assume $\ln A = 13.824 = \mathrm{const}$ (A in s^{-1}) and the temperature range is 973.15–1043.15 K (700–770 °C) [73], and according to Equation (14) we obtain $\Delta S^{+} = -148.13 \div -148.70$ J·mol^{-1}·K^{-1}. Assuming $\Delta S^{+} = -148$ J·mol^{-1}·K^{-1}, this value is practically consistent with that quoted in work [73].

In turn, for dynamic conditions, assuming $\ln A = 15.40 = \mathrm{const}$ (A in s^{-1}) (Table 1), the range of the conversion degree $\alpha = 0.1$–0.9, and seven heating rates $q = 1$–25 K·min^{-1}, ac-

cording to Equation (A9) we get $\Delta S^{+}\left(T_0 \rightarrow T_f\right) = -0.85 \div -1.0\ \mathrm{J{\cdot}mol^{-1}{\cdot}K^{-1}}$, i.e., $\Delta S^{+} \approx 0$. This result is valid only when $\ln A$ = const. For the variables $E = E(\alpha)$ and $A = A(\alpha)$, and according to Equations (A7) and (A8), different values will appear. It is most rational to test the significance of the KCE correlation and use Equation (A7).

Finally, for $\ln A$ = 15.4 (A in $\mathrm{s^{-1}}$), assuming in accordance with [67,68] (see Figure A5 in [67]) instead of the unknown isokinetic temperature, the measured harmonic mean temperature T_{iso} = 1023.07 K, then according to Equation (14) one obtains ΔS^{+}= −135.4 $\mathrm{J{\cdot}mol^{-1}{\cdot}K^{-1}}$ (see a_3 in Table 1).

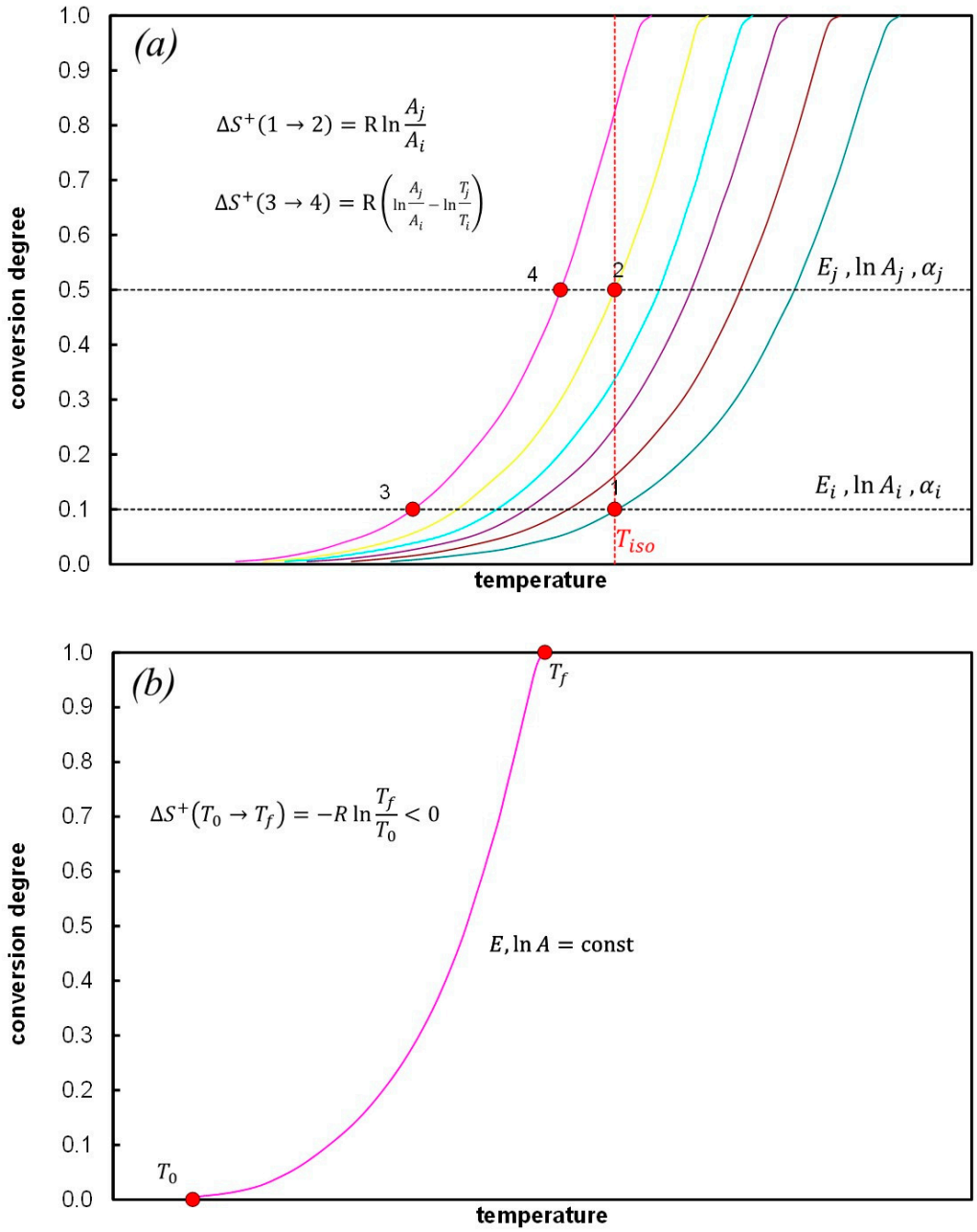


Figure A2. Interpretation of activation entropy for dynamic conditions in relation to the conversion degree vs. temperature: (**a**) for notation (A7) and (A8) for α = const, q = var, (**b**) for notation (A9) for α = var, q = const. Red points indicate characteristic points and characteristic temperatures in Equations (A7)–(A9).

References

1. Eyring, H. The Activated Complex in Chemical Reactions. *J. Chem. Phys.* **1935**, *3*, 107–115. [CrossRef]
2. Truhlar, D.G.; Garrett, B.C.; Klippenstein, S.J. Current Status of Transition-State Theory. *J. Phys. Chem.* **1996**, *100*, 12771–12800. [CrossRef]
3. Evans, M.G.; Polanyi, M. On the introduction of thermodynamic variables into reaction kinetics. *Trans. Faraday Soc.* **1937**, *33*, 448–452. [CrossRef]
4. Shannon, R.D. Activated complex theory applied to the thermal decomposition of solids. *Trans. Faraday Soc.* **1964**, *60*, 1902–1913. [CrossRef]
5. Garrett, B.C. Perspective on "The transition state method". *Theor. Chem. Acc.* **2000**, *103*, 200–204. [CrossRef] [PubMed]
6. Atanassov, A.; Genieva, S.; Vlaev, L. Study on the Thermooxidative Degradation Kinetics of Tetrafluoroethylene-Ethylene Copolymer Filled with Rice Husks Ash. *Polym. Technol. Eng.* **2010**, *49*, 541–554. [CrossRef]
7. Kim, Y.S.; Kim, Y.S.; Kim, S.H. Investigation of Thermodynamic Parameters in the Thermal Decomposition of Plastic Waste−Waste Lube Oil Compounds. *Environ. Sci. Technol.* **2010**, *44*, 5313–5317. [CrossRef] [PubMed]
8. Xu, Y.; Chen, B. Investigation of thermodynamic parameters in the pyrolysis conversion of biomass and manure to biochars using thermogravimetric analysis. *Bioresour. Technol.* **2013**, *146*, 485–493. [CrossRef]
9. Rony, A.H.; Kong, L.; Lu, W.; Dejam, M.; Adidharma, H.; Gasem, K.A.; Zheng, Y.; Norton, U.; Fan, M. Kinetics, thermodynamics, and physical characterization of corn stover (*Zea mays*) for solar biomass pyrolysis potential analysis. *Bioresour. Technol.* **2019**, *284*, 466–473. [CrossRef]
10. Sahoo, A.; Kumar, S.; Mohanty, K. A comprehensive characterization of non-edible lignocellulosic biomass to elucidate their biofuel production potential. *Biomass Convers. Biorefinery* **2020**, *12*, 5087–5103. [CrossRef]
11. Pinzi, S.; Buratti, C.; Bartocci, P.; Marseglia, G.; Fantozzi, F.; Barbanera, M. A simplified method for kinetic modeling of coffee silver skin pyrolysis by coupling pseudo-components peaks deconvolution analysis and model free-isoconversional methods. *Fuel* **2020**, *278*, 118260. [CrossRef]
12. Genieva, S.; Gonsalvesh, L.; Georgieva, V.; Tavlieva, M.; Vlaev, L. Kinetic analysis and pyrolysis mechanism of raw and impregnated almond shells. *Thermochim. Acta* **2021**, *698*, 178877. [CrossRef]
13. Banerjee, A.; Vithusha, T.; Krishna, B.B.; Kumar, J.; Bhaskar, T.; Ghosh, D. Pyrolysis of de-oiled yeast biomass of Rhodotorula mucilaginosa IIPL32: Kinetics and thermodynamic parameters using thermogravimetric analysis. *Bioresour. Technol.* **2021**, *340*, 125534. [CrossRef]
14. Patidar, K.; Singathia, A.; Vashishtha, M.; Sangal, V.K.; Upadhyaya, S. Investigation of kinetic and thermodynamic parameters approaches to non-isothermal pyrolysis of mustard stalk using model-free and master plots methods. *Mater. Sci. Energy Technol.* **2022**, *5*, 6–14. [CrossRef]
15. Tasar, S. Thermal conversion behavior of cellulose and hemicellulose fractions isolated from tea leaf brewing waste: Kinetic and thermodynamic evaluation. *Biomass Convers. Biorefinery* **2022**, *12*, 2935–2947. [CrossRef]
16. Sun, C.; Tan, H.; Zhang, Y. Simulating the pyrolysis interactions among hemicellulose, cellulose and lignin in wood waste under real conditions to find the proper way to prepare bio-oil. *Renew. Energy* **2023**, *205*, 851–863. [CrossRef]
17. Kissinger, H.E. Reaction Kinetics in Differential Thermal Analysis. *Anal. Chem.* **1957**, *29*, 1702–1706. [CrossRef]
18. Conner, W. A general explanation for the compensation effect: The relationship between $\Delta S^{\ddagger}_{+}$ and activation energy. *J. Catal.* **1982**, *78*, 238–246. [CrossRef]
19. Laidler, K.J.; King, M.C. The Development of transition-state theory. *J. Phys. Chem.* **1983**, *87*, 2657–2664. [CrossRef]
20. Hanggi, P.; Talkner, P.; Borkovec, M. Reaction-Rate Theory: Fifty Years After Kramers. *Rev. Mod. Phys.* **1990**, *62*, 251–341. [CrossRef]
21. Topaler, M.; Makri, N. Quantum rates for a double well coupled to a dissipative bath: Accurate path integral results and comparison with approximate theories. *J. Chem. Phys.* **1994**, *101*, 7500–7519. [CrossRef]
22. Rooney, J.J. Isokinetic temperature and the compensation effect in catalysis. *J. Mol. Catal. A Chem.* **1998**, *133*, 303–305. [CrossRef]
23. McBane, G.C.; de Levie, R.; Yan, Z.; Chang, Y.; Mayo, D.; Maslak, V.; Xia, S.; Badjić, J.D.; Williams, C.K.; Galley, W.C.; et al. Chemistry from Telephone Numbers: The False Isokinetic Relationship. *J. Chem. Educ.* **1998**, *75*, 919–922. [CrossRef]
24. Liu, L.; Guo, Q.-X. Isokinetic Relationship, Isoequilibrium Relationship, and Enthalpy−Entropy Compensation. *Chem. Rev.* **2001**, *101*, 673–696. [CrossRef]
25. Yelon, A.; Movaghar, B.; Crandall, R.S. Multi-excitation entropy: Its role in thermodynamics and kinetics. *Rep. Prog. Phys.* **2006**, *69*, 1145–1194. [CrossRef]
26. Principles of Chemical Kinetics-2nd Edition. Available online: https://www.elsevier.com/books/principles-of-chemical-kinetics/house/978-0-12-356787-1 (accessed on 14 March 2023).
27. Yelon, A.; Sacher, E.; Linert, W. Multi-Excitation Entropy, Entropy–Enthalpy Relations, and their Impact on Catalysis. *Catal. Lett.* **2011**, *141*, 954–957. [CrossRef]
28. Revell, L.E.; Williamson, B.E. Why Are Some Reactions Slower at Higher Temperatures? *J. Chem. Educ.* **2013**, *90*, 1024–1027. [CrossRef]
29. Yin, C.; Du, J. The power-law reaction rate coefficient for an elementary bimolecular reaction. *Phys. A Stat. Mech. Appl.* **2014**, *395*, 416–424. [CrossRef]

30. Carvalho-Silva, V.H.; Aquilanti, V.; de Oliveira, H.C.B.; Mundim, K.C. Deformed transition-state theory: Deviation from Arrhenius behavior and application to bimolecular hydrogen transfer reaction rates in the tunneling regime. *J. Comput. Chem.* **2016**, *38*, 178–188. [CrossRef]
31. Sanjeev, R.; Padmavathi, D.A.; Jagannadham, V. The 'Yard Stick' to Interpret the Entropy of Activation in Chemical Kinetics: A Physical-Organic Chemistry Exercise. *World J. Chem. Educ.* **2018**, *6*, 78–81. [CrossRef]
32. Khrapunov, S. The Enthalpy-entropy Compensation Phenomenon. Limitations for the Use of Some Basic Thermodynamic Equations. *Curr. Protein Pept. Sci.* **2018**, *19*, 1088–1091. [CrossRef]
33. Braun, A.; Chen, Q.; Yelon, A. Hole and Protonic Polarons in Perovskites. *Chimia* **2019**, *73*, 936–942. [CrossRef]
34. Sapunov, V.N.; Saveljev, E.A.; Voronov, M.S.; Valtiner, M.; Linert, W. The Basic Theorem of Temperature-Dependent Processes. *Thermo* **2021**, *1*, 45–60. [CrossRef]
35. Vyazovkin, S. Determining Preexponential Factor in Model-Free Kinetic Methods: How and Why? *Molecules* **2021**, *26*, 3077. [CrossRef]
36. Linert, W. The isokinetic relationship. X. Experimental examples to the relationship between isokinetic temperatures and active heat bath frequencies. *Chem. Phys.* **1989**, *129*, 381–393. [CrossRef]
37. Rooney, J. An explanation of isokinetic temperature in heterogeneous catalysis. *Catal. Lett.* **1998**, *50*, 15. [CrossRef]
38. Larsson, R. Catalysis as a resonance effect, V. Factors that determine the isokinetic temperature in catalytic reactions. *React. Kinet. Catal. Lett.* **1999**, *68*, 115–124. [CrossRef]
39. Armstrong, A.A.; Amzel, L.M. Role of Entropy in Increased Rates of Intramolecular Reactions. *J. Am. Chem. Soc.* **2003**, *125*, 14596–14602. [CrossRef]
40. Craig, I.R.; Thoss, M.; Wang, H. Proton transfer reactions in model condensed-phase environments: Accurate quantum dynamics using the multilayer multiconfiguration time-dependent Hartree approach. *J. Chem. Phys.* **2007**, *127*, 144503. [CrossRef]
41. Piskulich, Z.A.; Mesele, O.O.; Thompson, W.H. Activation Energies and Beyond. *J. Phys. Chem. A* **2019**, *123*, 7185–7194. [CrossRef]
42. Ivanova, Y.; Pukhovskaya, S.; Mamardashvili, N.; Koifman, O.; Kruk, M. Rate-acidity hysteresis and enthalpy-entropy compensation upon metalloporphyrin formation: Implication for the metal ion coordination mechanism. *J. Mol. Liq.* **2018**, *275*, 491–498. [CrossRef]
43. Odai, K.; Umesaki, K. Kinetic Study of Transition Mutations from G–C to A–T Base Pairs in Watson–Crick DNA Base Pairs: Double Proton Transfers. *J. Phys. Chem. A* **2021**, *125*, 8196–8204. [CrossRef]
44. Nakamura, S.; Sakai, H.; Fuki, M.; Kobori, Y.; Tkachenko, N.V.; Hasobe, T. Enthalpy–Entropy Compensation Effect for Triplet Pair Dissociation of Intramolecular Singlet Fission in Phenylene Spacer-Bridged Hexacene Dimers. *J. Phys. Chem. Lett.* **2021**, *12*, 6457–6463. [CrossRef]
45. Shpanko, I.V.; Sadovaya, I.V. Enthalpy–Entropy Compensation in Reactions of Oxirane Ring Opening. *Russ. J. Phys. Chem. A* **2022**, *96*, 2307–2317. [CrossRef]
46. Slocombe, L.; Winokan, M.; Al-Khalili, J.; Sacchi, M. Quantum Tunnelling Effects in the Guanine-Thymine Wobble Misincorporation via Tautomerism. *J. Phys. Chem. Lett.* **2022**, *14*, 9–15. [CrossRef]
47. Maciejewski, M.; Oswald, H.-R.; Reller, A. Thermal transformations of vaterite and calcite. *Thermochim. Acta* **1994**, *234*, 315–328. [CrossRef]
48. Mianowski, A.; Baraniec, I. Three-parametric equation in evaluation of thermal dissociation of reference compound. *J. Therm. Anal. Calorim.* **2009**, *96*, 179–187. [CrossRef]
49. Vyazovkin, S. When can the effect of thermal inertia be considered negligible? *Int. J. Chem. Kinet.* **2021**, *53*, 1058–1060. [CrossRef]
50. Galukhin, A.V.; Nikolaev, I.; Nosov, R.V.; Islamov, D.; Vyazovkin, S. Solvent-induced changes in the reactivity of tricyanate esters undergoing thermal polymerization. *Polym. Chem.* **2021**, *12*, 6179–6187. [CrossRef]
51. Bl·ażejowski, J.; Rak, J.; Gutowski, M. On the possibilities of theoretical analysis of kinetics of the thermal decomposition of solids. *J. Therm. Anal. Calorim.* **1995**, *43*, 45–55. [CrossRef]
52. Barin, I. *Thermochemical Data of Pure Substances*; VCH: Weinheim, Germany, 1997.
53. Brown, M.; Maciejewski, M.; Vyazovkin, S.; Nomen, R.; Sempere, J.; Burnham, A.; Opfermann, J.; Strey, R.; Anderson, H.; Kemmler, A.; et al. Computational aspects of kinetic analysis: Part A: The ICTAC kinetics project-data, methods and results. *Thermochim. Acta* **2000**, *355*, 125–143. [CrossRef]
54. Tagawa, H. Thermal decomposition temperatures of metal sulfates. *Thermochim. Acta* **1984**, *80*, 23–33. [CrossRef]
55. Warner, N.A.; Ingraham, T.R. Kinetic studies of the thermal decomposition of ferric sulphate and aluminum sulphate. *Can. J. Chem. Eng.* **1962**, *40*, 263–267. [CrossRef]
56. Coombs, P.G.; Munir, Z.A. The decomposition of iron(III) sulfate in air. *J. Therm. Anal.* **1989**, *35*, 967–976. [CrossRef]
57. Janković, B.; Stopić, S.; Bogović, J.; Friedrich, B. Kinetic and thermodynamic investigations of non-isothermal decomposition process of a commercial silver nitrate in an argon atmosphere used as the precursors for ultrasonic spray pyrolysis (USP): The mechanistic approach. *Chem. Eng. Process. Process. Intensif.* **2014**, *82*, 71–87. [CrossRef]
58. Bhatia, S.K.; Perlmutter, D.D. Effect of the product layer on the kinetics of the CO_2-lime reaction. *AIChE J.* **1983**, *29*, 79–86. [CrossRef]
59. Gupta, H.; Fan, L.-S. Carbonation−Calcination Cycle Using High Reactivity Calcium Oxide for Carbon Dioxide Separation from Flue Gas. *Ind. Eng. Chem. Res.* **2002**, *41*, 4035–4042. [CrossRef]

60. Fedunik-Hofman, L.; Bayon, A.; Donne, S.W. Comparative Kinetic Analysis of $CaCO_3$/CaO Reaction System for Energy Storage and Carbon Capture. *Appl. Sci.* **2019**, *9*, 4601. [CrossRef]
61. Brittain, R.D.; Hildenbrand, D.L. Catalytic decomposition of gaseous sulfur trioxide. *J. Phys. Chem.* **1983**, *87*, 3713–3717. [CrossRef]
62. Karasawa, H.; Sasahira, A.; Hoshino, K. Thermal decomposition of SO_3. *Int. J. Nucl. Hydrogen Prod. Appl.* **2006**, *1*, 134. [CrossRef]
63. Ishikawa, H.; Ishii, E.; Uehara, I.; Nakane, M. Catalyzed thermal decompositon of H2SO4 and production of HBr by the reaction of SO_2 with Br_2 and H_2O. *Int. J. Hydrogen Energy* **1982**, *7*, 237–246. [CrossRef]
64. GESTIS-Stoffdatenbank. Available online: https://gestis.dguv.de/data?name=003720&lang=en%20%20%202012-09-03 (accessed on 19 March 2023).
65. Ismael, S.; Deif, A.; Maraden, A.; Yehia, M.; Elbasuney, S. Ammonium perchlorate catalyzed with novel porous Mn-doped Co_3O_4 microspheres: Superior catalytic activity, advanced decomposition kinetics and mechanisms. *J. Therm. Anal. Calorim.* **2023**, *148*, 11811–11824. [CrossRef]
66. Krug, R.R. Detection of the Compensation Effect(θ Rule). *Ind. Eng. Chem. Fundam.* **1980**, *19*, 50–59. [CrossRef]
67. Mianowski, A.; Radko, T.; Bigda, R. Isokinetic and Compensation Temperature in the Analysis of Thermal Dissociation of the Solid Phase under Dynamic Conditions. *Energies* **2023**, *16*, 5692. [CrossRef]
68. Griessen, R.; Boelsma, C.; Schreuders, H.; Broedersz, C.P.; Gremaud, R.; Dam, B. Single Quality Factor for Enthalpy-Entropy Compensation, Isoequilibrium and Isokinetic Relationships. *Chemphyschem* **2020**, *21*, 1632–1643. [CrossRef] [PubMed]
69. Griessen, R.; Dam, B. Simple Accurate Verification of Enthalpy-Entropy Compensation and Isoequilibrium Relationship. *Chemphyschem* **2021**, *22*, 1774–1784. [CrossRef] [PubMed]
70. Janković, B.; Manić, N.; Perović, I.; Vujković, M.; Zdolšek, N. Thermal decomposition kinetics of deep eutectic solvent (DES) based on choline chloride and magnesium chloride hexahydrate: New details on the reaction mechanism and enthalpy–entropy compensation (EEC). *J. Mol. Liq.* **2023**, *374*, 121274. [CrossRef]
71. Schmitz, G.; Lente, G. Fundamental concepts in chemical kinetics. *ChemTexts* **2019**, *6*, 1. [CrossRef]
72. Vyazovkin, S.; Linert, W. Thermally induced reactions of solids: Isokinetic relationships of non-isothermal systems. *Int. Rev. Phys. Chem.* **1995**, *14*, 355–369. [CrossRef]
73. Mianowski, A.; Radko, T.; Siudyga, T. Kinetic compensation effect of isoconversional methods. *React. Kinet. Mech. Catal.* **2021**, *132*, 37–58. [CrossRef]
74. Langmuir, I. The Evaporation, Condensation and Reflection of Molecules and the Mechanism of Adsorption. *Phys. Rev. B* **1916**, *8*, 149–176. [CrossRef]
75. Britton, H.T.S.; Gregg, S.J.; Winsor, G.W. The calcination of dolomite. Part I.—The kinetics of the thermal decomposition of calcite and of magnesite. *Trans. Faraday Soc.* **1952**, *48*, 63–69. [CrossRef]
76. Šesták, J. Where did you come from and where are you heading to, thermal analysis of heating effects? *J. Therm. Anal. Calorim.* **2023**, *148*, 13141–13156. [CrossRef]
77. Lyon, R.E. A Physical Basis for Kinetic Compensation. *J. Phys. Chem. A* **2023**, *127*, 2399–2406. [CrossRef] [PubMed]
78. Šimon, P.; Dubaj, T.; Cibulková, Z. Frequent flaws encountered in the manuscripts of kinetic papers. *J. Therm. Anal. Calorim.* **2022**, *147*, 10083–10088. [CrossRef] [PubMed]
79. Vyazovkin, S. *Isoconversional Kinetics of Thermally Stimulated Processes*; Springer International Publishing: Berlin/Heidelberg, Germany, 2015. [CrossRef]
80. Sestak, J. *Thermal Analysis and Thermodynamic Properties of Solids*; Elsevier: Amsterdam, The Netherlands, 2021. [CrossRef]
81. Silva, V.H.; Aquilanti, V.; de Oliveira, H.C.; Mundim, K.C. Uniform description of non-Arrhenius temperature dependence of reaction rates, and a heuristic criterion for quantum tunneling vs classical non-extensive distribution. *Chem. Phys. Lett.* **2013**, *590*, 201–207. [CrossRef]
82. Starikov, E. Valid entropy–enthalpy compensation: Fine mechanisms at microscopic level. *Chem. Phys. Lett.* **2013**, *564*, 88–92. [CrossRef]
83. Chakraborty, H.; Tarafdar, P.K.; Bruno, M.J.; Sengupta, T.; Lentz, B.R. Activation Thermodynamics of Poly(Ethylene Glycol)-Mediated Model Membrane Fusion Support Mechanistic Models of Stalk and Pore Formation. *Biophys. J.* **2012**, *102*, 2751–2760. [CrossRef]
84. Sronsri, C.; Noisong, P.; Danvirutai, C. Isoconversional kinetic, mechanism and thermodynamic studies of the thermal decomposition of $NH_4Co_{0.8}Zn_{0.1}Mn_{0.1}PO_4{\cdot}H_2O$. *J. Therm. Anal. Calorim.* **2015**, *120*, 1689–1701. [CrossRef]
85. Sronsri, C.; Danvirutai, C.; Noisong, P. Double function method for the confirmation of the reaction mechanism of $LiCoPO_4$ nanoparticle formation, reliable activation energy, and related thermodynamic functions. *React. Kinet. Catal. Lett.* **2017**, *121*, 555–577. [CrossRef]
86. Sronsri, C.; Boonchom, B. Thermal kinetic analysis of a complex process from a solid-state reaction by deconvolution procedure from a new calculation method and related thermodynamic functions of $Mn_{0.9}0Co_{0.05}Mg_{0.05}HPO_4{\cdot}3H_2O$. *Trans. Nonferrous Met. Soc. China* **2018**, *28*, 1887–1902. [CrossRef]

Disclaimer/Publisher's Note: The statements, opinions and data contained in all publications are solely those of the individual author(s) and contributor(s) and not of MDPI and/or the editor(s). MDPI and/or the editor(s) disclaim responsibility for any injury to people or property resulting from any ideas, methods, instructions or products referred to in the content.